

A Short Nur77-Derived Peptide Converts Bcl-2 from a Protector to a Killer

Siva Kumar Kolluri,^{1,2,5} Xiuwen Zhu,^{1,5} Xin Zhou,¹ Bingzhen Lin,¹ Ya Chen,¹ Kai Sun,¹ Xuefei Tian,³ James Town,¹ Xihua Cao,¹ Feng Lin,¹ Dayong Zhai,¹ Shinichi Kitada,¹ Frederick Luciano,¹ Edmond O'Donnell,² Yu Cao,¹ Feng He,³ Jialing Lin,³ John C. Reed,¹ Arnold C. Satterthwait,^{1,*} and Xiao-kun Zhang^{1,4,*}

¹Cancer Center, Burnham Institute for Medical Research, La Jolla, CA 92037, USA

²Cancer Biology Laboratory, Department of Environmental and Molecular Toxicology, Oregon State University, Corvallis, OR 97331, USA

³Department of Biochemistry and Molecular Biology, University of Oklahoma Health Sciences Center, Oklahoma City, OK 73126, USA

⁴Institute for Biomedical Research, Xiamen University, Xiamen 361005, China

⁵These authors contributed equally to this work

*Correspondence: asat@burnham.org (A.C.S.), xzhang@burnham.org (X.-k.Z.)

DOI 10.1016/j.ccr.2008.09.002

SUMMARY

Bcl-2 can be converted into a proapoptotic molecule by nuclear receptor Nur77. However, the development of Bcl-2 converters as anticancer therapeutics has not been explored. Here we report the identification of a Nur77-derived Bcl-2-converting peptide with 9 amino acids (NuBCP-9) and its enantiomer, which induce apoptosis of cancer cells in vitro and in animals. The apoptotic effect of NuBCPs and their activation of Bax are not inhibited but rather potentiated by Bcl-2. NuBCP-9 and its enantiomer bind to the Bcl-2 loop, which shares the characteristics of structurally adaptable regions with many cancer-associated and signaling proteins. NuBCP-9s act as molecular switches to dislodge the Bcl-2 BH4 domain, exposing its BH3 domain, which in turn blocks the activity of antiapoptotic Bcl-X_L.

INTRODUCTION

Members of the Bcl-2 family are critical regulators of apoptosis, an important biological process that eliminates cells with increased malignant potential such as those with damaged DNA or aberrant cell cycling (Cory et al., 2003; Green and Kroemer, 2004; Reed, 1998; Vander Heiden and Thompson, 1999). They possess at least one of four conserved motifs called Bcl-2 homology (BH) domains. The family is divided into three subclasses based on the number of BH domains and their function: the antiapoptotics, including Bcl-2 and Bcl-X_L, which possess sequence conservation through BH1–4; the multidomain proapoptotics, such as Bax and Bak, which possess BH1–3; and the BH3-only proapoptotic molecules such as Bid, Bim, and Bad (Cory et al., 2003; Green and Kroemer, 2004; Reed, 1998; Vander Heiden and Thompson, 1999). The Bcl-2 family regulates apoptosis through interactions between its proapoptotic and antiapoptotic family members. BH3-only proteins convey diverse death signals by directly or indirectly activating Bax and/or

Bak, which can induce permeabilization of the outer mitochondrial membrane and release apoptogenic factors needed to activate the caspases (Kuwana et al., 2005; Leber et al., 2007; Letai et al., 2002; Willis and Adams, 2005; Willis et al., 2007). Antiapoptotic family members inhibit death by restraining Bax and Bak activity and/or sequestering BH3-only members. Approaches targeting prosurvival Bcl-2 family members, such as BH3 domain-derived peptides or chemical inhibitors such as ABT-737 (Bouillet and Strasser, 2002; Degtarev et al., 2001; Oltersdorf et al., 2005; Reed, 2002; Walensky et al., 2004), are being developed, which show significant anticancer activities. These BH3 peptides and chemical inhibitors act by binding to the hydrophobic groove formed by the BH1–3 domains of the prosurvival proteins and antagonizing their survival function, resulting in release of proapoptotic members that activate apoptosis.

The functional phenotype of some Bcl-2 family members such as Bcl-2 can be reversed in some cellular contexts. For example, mutants of the Bcl-2-homolog *Ced-9* appear to promote rather than prevent apoptosis in *C. elegans* (Xue and Horvitz, 1997).

SIGNIFICANCE

We report that a Nur77-based peptide and its enantiomer bind to the Bcl-2 loop, converting Bcl-2 from a protector to a killer of cancer cells. Our results provide mechanistic insight into Bcl-2 conversion and identify a new direction for Bcl-2-based drug leads and cancer drug development. These findings should appeal to a broad audience of clinicians, cancer biologists, molecular biologists, and drug designers who have followed therapeutic approaches targeting Bcl-2 and the underlying molecular mechanisms. In addition, peptide and protein chemists and structural biologists will be intrigued by the activity of the NuBCP-9 enantiomer, which has important mechanistic implications with broad potential for cancer therapeutics.

Likewise, Bcl-2 homologs in *Drosophila* can manifest either cytoprotective or cytodestructive phenotypes, depending on cellular context (Colussi et al., 2000; Igaki et al., 2000). The mechanisms responsible for the phenotypic conversion of Bcl-2 are largely undefined. However, the unstructured loop of Bcl-2, which links the BH3 and BH4 domains, appears important (Moll et al., 2006; Zhang, 2007). When the Bcl-2 loop is cleaved by caspase-3, Bcl-2 is converted to a proapoptotic protein similar to Bax (Cheng et al., 1997; Grandgirard et al., 1998). Phosphorylation of the loop has also been speculated to convert Bcl-2 to a proapoptotic form (Blagosklonny, 2001). It inhibits binding of Bcl-2 to multidomain and BH3-only proapoptotic family members (Bassik et al., 2004) and the autophagic protein beclin 1 (Wei et al., 2008). We recently reported that nuclear receptor Nur77 converts Bcl-2 into a killer by binding its loop (Lin et al., 2004). Nur77 (also called TR3 or NGFI-B) is a potent proapoptotic member of the nuclear receptor superfamily (Moll et al., 2006; Zhang, 2007). It often translocates from the nucleus to mitochondria in response to different death signals, where it binds Bcl-2, inducing a conformational change (Li et al., 2000; Lin et al., 2004). Nur77 translocation to mitochondria and its induction of a Bcl-2 conformational change have also been implicated in the negative selection of thymocytes in vitro and in animals (Thompson and Winoto, 2008), indicating a physiological role for the Nur77-Bcl-2 interaction. Interestingly, p53 also binds the Bcl-2 loop (Moll et al., 2006), which then acts like a BH3-only protein to activate Bax or Bak by releasing BH3-only proteins such as Bid (Chipuk et al., 2005; Leu et al., 2004; Mihara et al., 2003).

The apoptotic effect of Nur77 appears to be clinically relevant, as the expression of the Nur77 subfamily member Nor-1 is positively correlated with survival of diffuse large B cell lymphoma patients (Shipp et al., 2002) and Nur77 downregulation is associated with metastasis of several primary solid tumors (Ramaswamy et al., 2003). Thus, targeting the Nur77-Bcl-2 apoptotic pathway is an attractive approach for developing cancer therapeutics. The ability of Nur77 to convert Bcl-2 distinguishes this death protein from proapoptotic Bcl-2 family proteins, whose activities are restrained by prosurvival Bcl-2 family members. It also offers an opportunity to design drugs that are likely to be effective against cancer cells with high Bcl-2 levels. Here, we report the identification of a short Nur77-derived peptide and its enantiomer that act as molecular switches to induce a Bcl-2 conformational change, converting it from a protector to a killer of cancer cells in vitro and in animals.

RESULTS

A 9 Amino Acid Peptide from Nur77 Induces Apoptosis

To develop Bcl-2 converters that induce apoptosis in cancer cells with high Bcl-2 levels, peptides corresponding to subregions of a Nur77 fragment known to interact with Bcl-2 (Lin et al., 2004) were synthesized and conjugated with the cell-penetrating peptide (CPP) D-Arg octamer (r8) (Jones et al., 2005) (Figure 1A). Among these, a 20 amino acid peptide (aa 480–499) (NuBCP-20) exhibited potent apoptotic effect in various cancer cell lines, being more potent than a BH3 peptide derived from the proapoptotic Bcl-2 family member Bid (Letai et al., 2002) (see Figures S1 and S2 available online). Serial deletion identified a 9 aa Nur77 peptide, NuBCP-9, which effectively in-

duced apoptosis of breast cancer cells (Figure 1B; Figure S2). Neither NuBCP-20 nor NuBCP-9 induced apoptosis of normal primary mammary epithelial cells (Figure 1B; Figure S1). NuBCP-9 is considerably shorter than the shortest BH3 peptide that binds Bcl-2. Further deletion from either its N-terminal or C-terminal end or substituting Ala for the NuBCP-9 terminal amino acids (NuBCP-9/AA) completely abolished its apoptotic effect (Figure S2). NuBCP-9 linked to other CPPs, penetratin, or transportan 10 (Jones et al., 2005) as well as r8 by a disulfide bond exhibited a similar degree of apoptosis (Figure S2). Since disulfide bonds are rapidly reduced in cells, the apoptotic effect of NuBCP-9 is not due to its linkage with CPPs.

While investigating the sequence requirements for NuBCP-9, we discovered that replacing L-amino acids with D-amino acids did not diminish its apoptotic effect. Peptide enantiomers have been reported to interact with several proteins (Zhou et al., 2002), including calmodulin, $\alpha 3\beta 1$ integrin, DnaJ (Hsp40) cochaperone, and CXCR4, which like Bcl-2 are characterized by large natively disordered loops. In contrast, the enantiomer of Bad BH3 peptide was not apoptotic (Figure 1C), demonstrating different modes of action of the NuBCP-9 and Bad BH3 peptides.

Induction of Apoptosis by NuBCP-9 Is Bcl-2 Dependent

We next examined whether NuBCP-9-induced apoptosis is dependent on Bcl-2 expression. NuBCP-9 and its enantiomer showed little effect on Jurkat cells (<20% apoptosis). However, both peptides induced extensive apoptosis (>50%) in Jurkat cells stably expressing Bcl-2 (Figure 1D). In contrast, apoptosis induced by staurosporine (STS) and Bid BH3 peptide was attenuated by Bcl-2 overexpression in Jurkat cells (Figure S3), demonstrating the dual role of Bcl-2. Stable expression of Bcl-2 in CEM leukemia cells also potentiated the apoptotic effect of Nur77 peptide but prevented the killing by STS and Bad BH3 peptide (Figure S4). The apoptotic effect of NuBCP-9 was further evaluated in mouse embryonic fibroblasts (MEFs) and Bcl-2 knockout MEFs (*Bcl-2*^{-/-} MEFs). Although the apoptotic effect of STS and Bad BH3 peptide was enhanced in *Bcl-2*^{-/-} MEFs (Figure 1E), NuBCP-9 and D-NuBCP-9 induced apoptosis of wild-type MEFs but not *Bcl-2*^{-/-} MEFs in a dose-dependent (Figure 1F) and time-dependent (Figure 1G) manner. Furthermore, suppression of Bcl-2 expression by siRNA or antisense oligonucleotides reduced the killing effect of NuBCP-9 enantiomers (Figures S5 and S6). Thus, Bcl-2 is a major target of NuBCP-9s. NuBCP-induced apoptosis requires Bax or Bak, as the peptides induced apoptosis similarly in wild-type, *Bax*^{-/-}, and *Bak*^{-/-} MEFs but lacked activity in double-knockout *Bax*^{-/-} *Bak*^{-/-} MEFs (Figure 1H), further demonstrating that the peptides act via the Bcl-2-regulated pathway.

The effects of Nur77 peptides on clonogenic survival of MEFs were determined. After exposure to NuBCP-9 or D-NuBCP-9 peptide, wild-type MEFs formed very few colonies compared to *Bcl-2*^{-/-} MEFs (Figure 2A). For example, wild-type MEFs treated with 10 μ M D-NuBCP-9 formed only 5% as many colonies as *Bcl-2*^{-/-} MEFs. The suppressive effect of NuBCP-9 (Figure 2B) or D-NuBCP-9 (Figure 2C) was also largely reduced in *Bax*^{-/-} *Bak*^{-/-} MEFs. Treatment with 15 μ M D-NuBCP-9 resulted in approximately 80% reduction of colonies in wild-type MEFs but did not decrease the number of colonies formed by *Bax*^{-/-} *Bak*^{-/-} MEFs (Figure 2C). To further evaluate NuBCPs,

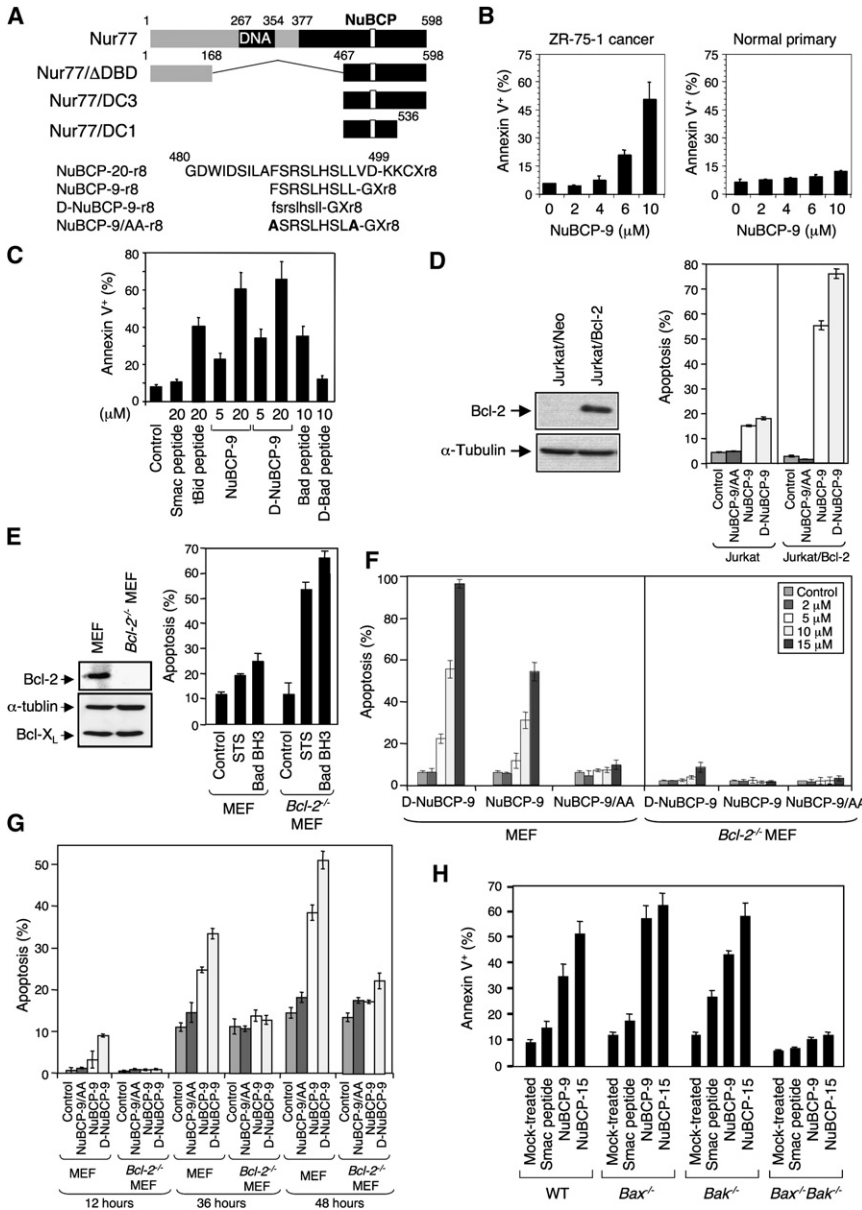


Figure 1. Apoptosis Induction by NuBCP

(A) Location of NuBCP in Nur77, Nur77 mutants, and peptide sequences used in this study. Amino acids (aa) are given in single-letter code, with upper case for L-aa and lower case for D-aa. X, N-aminocaproic acid; CX, covalent linkage between cysteine thiol and acetyl group. Mutated aa are bolded. Peptides conjugated with polyarginine (r8) were used in all studies unless otherwise indicated.

(B) NuBCP-9 induces apoptosis in ZR-75-1 breast cancer cells, but not in normal primary mammary epithelial cells. Cells were exposed to NuBCP-9 for 24 hr, and apoptosis was determined by annexin V staining.

(C) Apoptotic effect of NuBCP-9 is retained in its enantiomer. H460 cells were exposed to the indicated peptide for 24 hr, and apoptosis was determined by annexin V staining.

(D) Bcl-2-dependent apoptosis induction by NuBCP-9s in Jurkat cells. Left panel: Bcl-2 expression in Jurkat cells transfected with neo control vector (Jurkat/Neo) or Bcl-2 expression vector (Jurkat/Bcl-2) was determined by immunoblotting. Right panel: cells were exposed to NuBCP-9s (10 μ M) in medium containing 5% FBS for 36 hr, and apoptosis was determined by DAPI staining.

(E) Knockout of Bcl-2 enhances the apoptotic effect of staurosporine (STS) and Bad BH3 peptide. Left panel: Bcl-2 expression in wild-type MEFs and *Bcl-2*^{-/-} MEFs was determined by immunoblotting. Right panel: apoptosis of cells exposed to STS (0.1 μ M) or Bad BH3 peptide (10 μ M) for 36 hr was determined by DAPI staining.

(F) Dose-dependent apoptosis induction by NuBCP-9s in wild-type MEFs and *Bcl-2*^{-/-} MEFs. Cells (10,000 per well) were seeded in medium containing 5% FBS and then exposed to the indicated concentration of NuBCP-9 peptides conjugated with penetratin peptide (NuBCP-9-pen) (Figure S2) for 36 hr. Apoptosis was determined by DAPI staining.

(G) Time-course analysis of apoptosis induction by NuBCP-9s in wild-type MEFs and *Bcl-2*^{-/-} MEFs. Cells (15,000 per well) seeded in medium containing 5% FBS were exposed to the indicated NuBCP-9-pen (10 μ M) for the indicated period of time. Apoptosis was determined by DAPI staining.

(H) Bax or Bak is required for apoptotic effect of NuBCPs. The indicated types of MEF were exposed to peptide (15 μ M) for 36 hr, and apoptosis was determined by annexin V staining.

In (B)–(H), the bars represent means \pm SD from three or four experiments.

their effects on the growth of tumors formed in severe combined immunodeficiency (SCID) mice were examined. Injection of L- or D-NuBCP-9, but not control peptide (NuBCP-9/AA), dramatically suppressed the growth of MDA-MB435 cancer cell xenografts in mice (Figure 2D; Figure S2C) and potentially induced apoptosis of tumor cells as revealed by TUNEL staining (Figures 2E and 2F). Furthermore, D-NuBCP-9 induced regression of tumors (Figure 2G). Thus, NuBCP-9 and its enantiomer effectively induce apoptosis in vitro and in animals, demonstrating their therapeutic potential.

NuBCP-9 and Its Enantiomer Bind Bcl-2

To determine whether NuBCPs bind Bcl-2, cDNAs encoding the residues 478–504 (Nur77/478–504) and 489–497 (Nur77/489–497, equivalent to NuBCP-9) of Nur77 were fused with green fluorescent protein (GFP) cDNA. When transfected into HEK293T cells, GFP-fused Nur77 fragments were precipitated by anti-Bcl-2 antibody only when Bcl-2 was coexpressed (Figure 3A). The coprecipitation was inhibited by addition of NuBCP-9, but not Smac peptide (data not shown). To study whether D-NuBCP-9 interacts with Bcl-2, we used

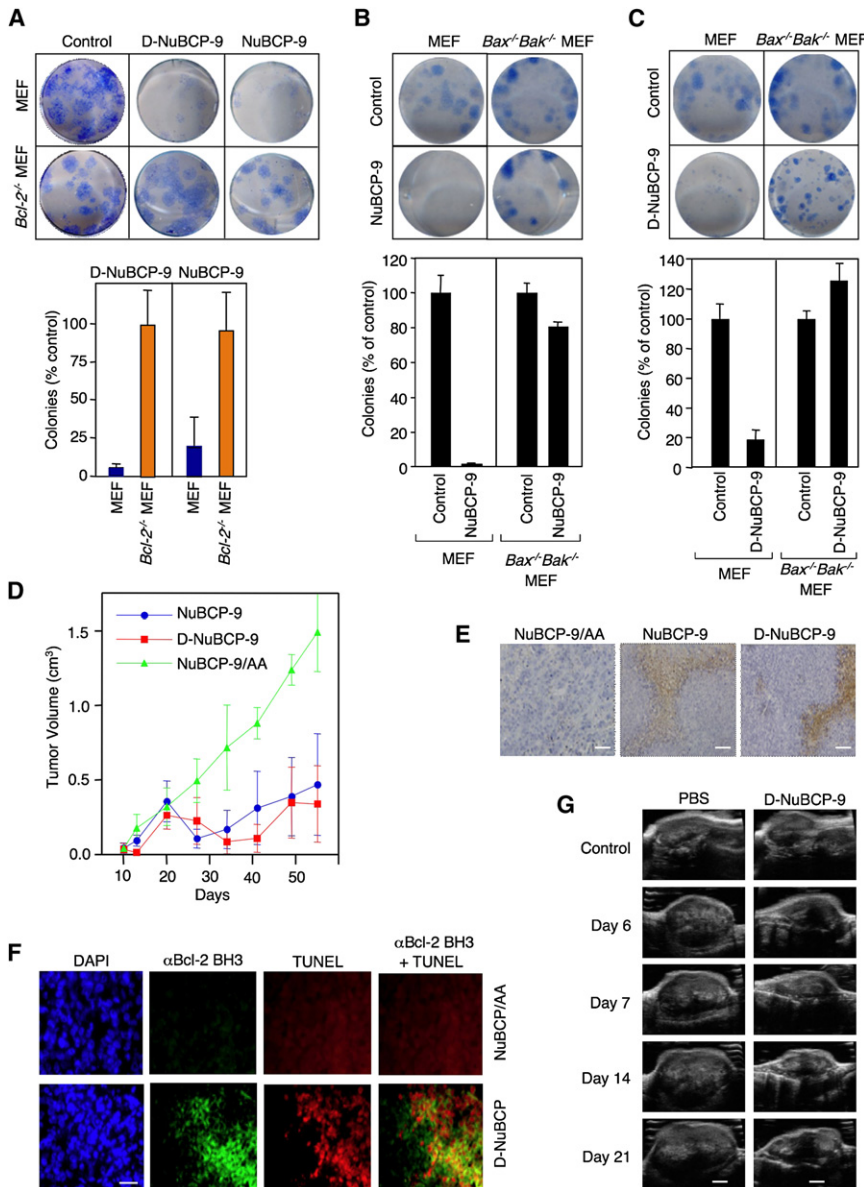


Figure 2. Antitumorigenic Effects of NuBCP-9s

(A) Effect of NuBCP-9s (10 μ M) on clonogenic survival of wild-type MEFs and *Bcl-2*^{-/-} MEFs. (B) Effect of NuBCP-9 (20 μ M) on clonogenic survival of wild-type MEFs and *Bax*^{-/-} *Bak*^{-/-} MEFs. (C) Effect of D-NuBCP-9 (15 μ M) on clonogenic survival of wild-type MEFs and *Bax*^{-/-} *Bak*^{-/-} MEFs.

Cells in (A)–(C) were exposed to the indicated concentrations of NuBCP-9-pen, D-NuBCP-9-pen, or NuBCP-9/AA-pen (Control). Data in (A)–(C) are means \pm SD from triplicate experiments.

(D) Inhibition of tumor growth by NuBCPs. MDA-MB435 tumors grown in SCID mice (n = 5) were injected with the indicated peptide, and tumor volumes were measured. Data are presented as mean \pm SD.

(E) Induction of apoptosis of tumor cells by NuBCPs. Tumor tissues from animals treated with the indicated peptide were stained by TUNEL for detection of apoptosis. Scale bar = 100 μ m.

(F) Correlation of apoptosis induction and Bcl-2 conformational change in vivo. Apoptosis in tumor tissues from animals treated for 2 days with peptide was determined by TUNEL staining. Conformational change in Bcl-2 was detected in the same tissues by immunostaining with anti-Bcl-2 BH3 domain antibody. Nuclei were visualized by DAPI staining. Scale bar = 100 μ m.

(G) Representative ultrasound images of established tumors injected with D-NuBCP-9. MDA-MB435 tumors (about 0.6 cm² in size) grown in SCID mice were injected with PBS or D-NuBCP-9-pen, and tumors were monitored by ultrasound technology (VisualSonics Inc.). Scale bar = 125 mm.

(G) Representative ultrasound images of established tumors injected with D-NuBCP-9. MDA-MB435 tumors (about 0.6 cm² in size) grown in SCID mice were injected with PBS or D-NuBCP-9-pen, and tumors were monitored by ultrasound technology (VisualSonics Inc.). Scale bar = 125 mm.

(G) Representative ultrasound images of established tumors injected with D-NuBCP-9. MDA-MB435 tumors (about 0.6 cm² in size) grown in SCID mice were injected with PBS or D-NuBCP-9-pen, and tumors were monitored by ultrasound technology (VisualSonics Inc.). Scale bar = 125 mm.

(G) Representative ultrasound images of established tumors injected with D-NuBCP-9. MDA-MB435 tumors (about 0.6 cm² in size) grown in SCID mice were injected with PBS or D-NuBCP-9-pen, and tumors were monitored by ultrasound technology (VisualSonics Inc.). Scale bar = 125 mm.

(G) Representative ultrasound images of established tumors injected with D-NuBCP-9. MDA-MB435 tumors (about 0.6 cm² in size) grown in SCID mice were injected with PBS or D-NuBCP-9-pen, and tumors were monitored by ultrasound technology (VisualSonics Inc.). Scale bar = 125 mm.

(G) Representative ultrasound images of established tumors injected with D-NuBCP-9. MDA-MB435 tumors (about 0.6 cm² in size) grown in SCID mice were injected with PBS or D-NuBCP-9-pen, and tumors were monitored by ultrasound technology (VisualSonics Inc.). Scale bar = 125 mm.

a competition assay. Nur77 lacking its DNA-binding domain (DBD), Nur77/ Δ DBD, bound Bcl-2 (Lin et al., 2004), and binding was inhibited by NuBCP-9 or D-NuBCP-9 (Figure 3B). GFP-Nur77/478–504 also bound to the antiapoptotic Bcl-2 family members Bcl-B and Bfl-1, but not Bcl-X_L or Mcl-1 (Figure 3C). Like Nur77 protein (Luciano et al., 2007), the killing effect of NuBCP-9 was enhanced by overexpression of Bcl-B in HeLa cells and inhibited by suppression of Bcl-B expression by siRNA in H460 cells (Figure S6). These results suggest that NuBCP-9 also converts Bcl-B into a proapoptotic molecule.

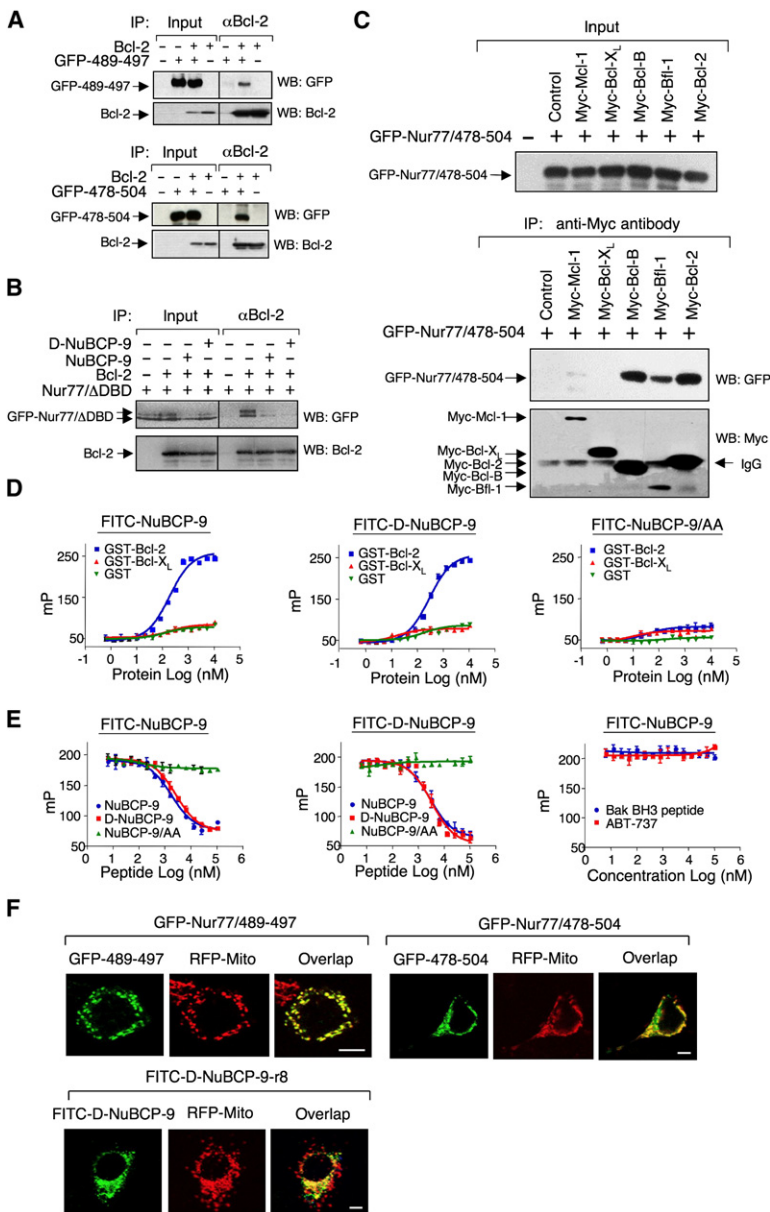
We next used fluorescence polarization (FP) assays to determine whether NuBCP-9s bind Bcl-2. GST-Bcl-2, but neither GST-Bcl-X_L nor GST, induced a concentration-dependent FP of FITC-NuBCP-9 and FITC-D-NuBCP-9, while the FP of FITC-NuBCP-9/AA was little affected (Figure 3D). In addition, unconjugated NuBCP-9 and D-NuBCP-9 competed with binding of

BH3 peptides, as shown by the failure of either a BH3 peptide (Bak BH3) or a potent small-molecule inhibitor (ABT-737) that targets the Bcl-2 BH3-binding site to reduce FITC-NuBCP-9 binding to GST-Bcl-2 (Figure 3E).

The GFP-Nur77/489–497 and GFP-Nur77/478–504 fusions colocalized extensively with RFP-Mito, a red fluorescent protein (RFP) fused to a mitochondria-targeting sequence (Figure 3F). FITC-D-NuBCP-9-r8 also displayed significant colocalization with RFP-Mito. Thus, NuBCP-9 and its enantiomer, like Nur77, bind Bcl-2 and target mitochondria.

NuBCP-9s Induce Bcl-2 Conformational Change

Conversion of Bcl-2 involves a conformational change that exposes its BH3 domain (Lin et al., 2004). BH3 domain exposure is detectable with an antibody against Bcl-2 BH3 peptide (Figure S7). The effect of NuBCPs on Bcl-2 conformation was examined by immunoprecipitation assays (Figure 4A).



The Bcl-2 BH3 domain antibody precipitated endogenous Bcl-2 in cells treated with NuBCP-9 or D-NuBCP-9, but not NuBCP-9/AA, showing that NuBCP-9s induce a Bcl-2 conformational change. In contrast, tBid BH3 and Bad BH3 peptides did not induce this effect, despite their induction of apoptosis. This was confirmed by flow cytometry analysis, which showed a strong enhancement in fluorescence upon staining with BH3 antibody of cells exposed to NuBCP-9s, but not NuBCP-9/AA, tBid BH3, or Smac peptide (Figure 4B). NuBCP-9-induced Bcl-2 BH3 domain immunofluorescence was observed in the presence of the caspase inhibitor zVAD, excluding the involvement of caspases in the Bcl-2 conformational change (Figure S7D). The NuBCP-induced Bcl-2 conformational change was also observed in solid tumors (Figure 2F). The overlapping of TUNEL staining with Bcl-2 BH3 immunofluorescence in tumors treated with NuBCP-9 (Figure 2F) is consistent

Figure 3. NuBCPs Interact with Bcl-2 and Target Mitochondria

(A) HEK293T cells transfected with GFP-Nur77/489-497 or GFP-Nur77/478-504 (2 μg) together with or without Bcl-2 expression plasmid (0.8 μg) were analyzed by coimmunoprecipitation (CoIP) using anti-Bcl-2 antibody, followed by western blotting (WB) using either anti-GFP or anti-Bcl-2 antibody (Lin et al., 2004). Cells were transfected in six-well plates at 80% confluency.

(B) HEK293T cells transfected with GFP-Nur77/ΔDBD and Bcl-2 were exposed to NuBCP-9 or D-NuBCP-9, and interaction was analyzed by CoIP.

(C) Interaction of NuBCP with antiapoptotic Bcl-2 family members, Bcl-B, Bfl-1, and Bcl-2. HEK293T cells in six-well plates transfected with GFP-Nur77/478-504 (2 μg) together with or without the indicated Myc-tagged Bcl-2 family member expression plasmids (0.8 μg) were analyzed by CoIP, followed by WB.

Input in (A)–(C) represents 5% of cell lysates used in the CoIP assays. Data from one of three experiments are shown.

(D) Fluorescence polarization (FP) assay of binding of NuBCPs to Bcl-2. GST-Bcl-2, GST-Bcl-X_L, or GST protein (200 nM) was incubated with the indicated FITC-NuBCP-r8 (20 nM) in triplicate in PBS (pH 7.6) at 25°C, and FP was determined when the signal stabilized within 20 min. Data are presented as mean ± SD.

(E) FP competition assay. GST-Bcl-2 protein (200 nM) was incubated with the indicated FITC-NuBCP-r8 (20 nM) in the presence or absence of unlabeled NuBCPs in triplicate in PBS (pH 7.6) at 25°C, and FP was determined when the signal stabilized within 20 min. Data are presented as mean ± SD.

(F) NuBCPs target mitochondria. RFP-Mito (50 ng) was transfected into H460 cells on glass coverslips together with GFP-Nur77/489-497 or GFP-Nur77/478-504 (50 ng) for 12 hr, or RFP-Mito was transfected into H460 cells for 12 hr and treated with 6 μM FITC-D-NuBCP-9-r8 for 2 hr, and subcellular localization of the fluorophores was analyzed by confocal microscopy. Approximately 10%–15% of GFP-fusion-transfected or FITC-D-NuBCP-9-treated cells displayed the localization shown. Scale bar = 4 μm.

with the notion that NuBCP-9-induced Bcl-2-dependent apoptosis is correlated with exposure of the Bcl-2 BH3 domain.

We next determined whether NuBCPs can induce a conformational change of purified GST-Bcl-2 protein using circular dichroism (CD) analysis. Our results showed similar changes in GST-Bcl-2 protein spectra when it was incubated with NuBCP-9 or D-NuBCP-9, but not NuBCP-9/AA (Figure 4C; Figure S8). The fact that NuBCP-9 and D-NuBCP-9 display mirror image spectra (Figures S8–S10) while inducing identical changes in the Bcl-2 spectra (Figure 4C; Figure S8) indicates that NuBCP-9 and D-NuBCP-9 do not contribute significantly to the spectral changes. Binding is saturable and stoichiometric with a K_d of 2.1 ± 0.2 μM for NuBCP-9 and 2.0 ± 0.1 μM for D-NuBCP-9 (Figures 4D and 4E), in agreement with FP assays (Figure 3E). In contrast, NuBCP-9, D-NuBCP-9, and NuBCP-9/AA had no effect on CD spectra for GST or GST-Bcl-X_L (Figures S9 and S10). Thus, the NuBCP-induced Bcl-2 conformational change observed in cells can be accounted for by direct binding of NuBCPs to Bcl-2 in a specific 1:1 complex.

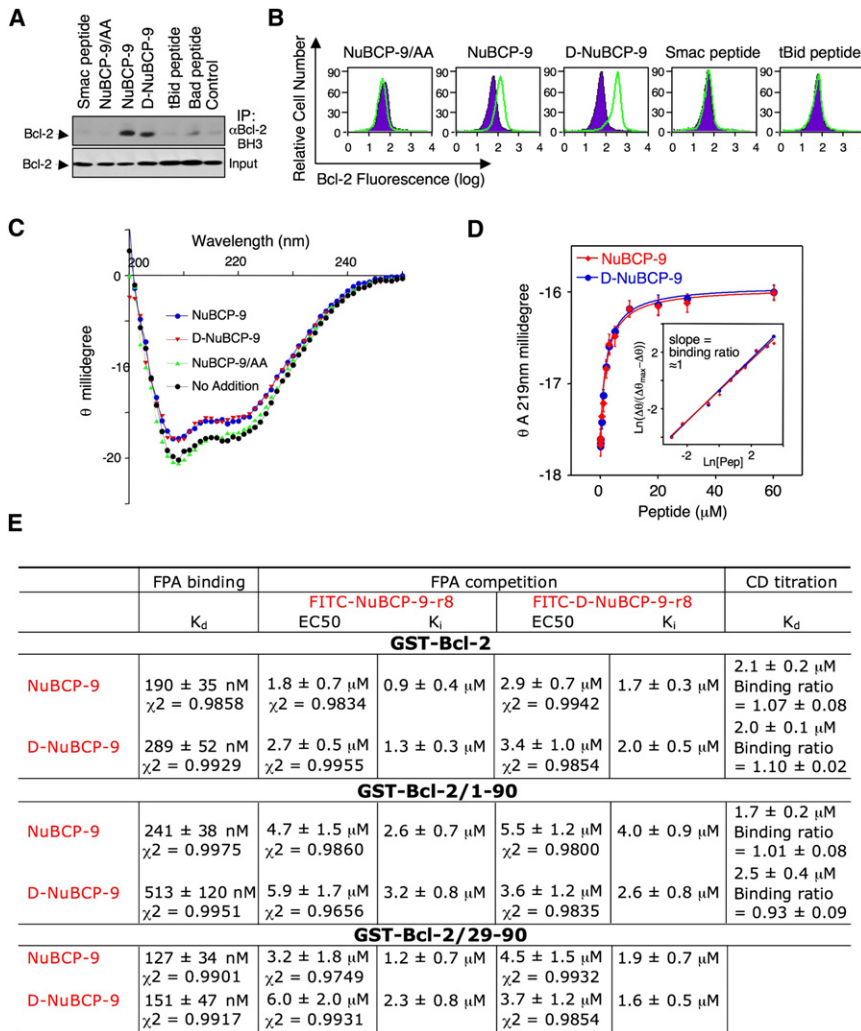


Figure 4. NuBCPs Induce Bcl-2 Conformational Change

(A) H460 cells were exposed to the indicated peptide (20 μ M) for 12 hr, and endogenous Bcl-2 was immunoprecipitated by anti-Bcl-2 BH3 domain antibody, followed by WB using a polyclonal anti-Bcl-2 antibody against the whole protein. Input represents 10% of lysates used for IP.

(B) Flow cytometry analysis of endogenous Bcl-2 immunofluorescence. H460 cells were treated as in (A) and immunostained with anti-Bcl-2 BH3 domain antibody (Abgent) and SRPD-conjugated secondary antibody (Southern Biotech). Bcl-2 fluorescence from peptide-treated cells (green histogram) was compared to that from the untreated cells (purple histogram).

(C) Circular dichroism (CD) spectra for the binding of NuBCP-9s (30 μ M) to GST-Bcl-2 (2 μ M) in PBS (pH 7.6) at 25°C. Data from one of three experiments are shown.

(D) Stoichiometry of binding of NuBCP-9 to GST-Bcl-2. GST-Bcl-2 was titrated with NuBCP-9s in PBS (pH 7.6) at 25°C. CD was taken at 219 nm, where absorption from the free peptide is <0.3% of protein. Stoichiometry was determined as described previously (Jones et al., 2002). Data are presented as mean \pm SD.

(E) Summary of binding of NuBCP-9 and its enantiomer to Bcl-2 and Bcl-2 mutants. $K_d \pm$ SD values for FITC-NuBCP-9-r8s binding GST-Bcl-2, GST-Bcl-2/1-90, or GST-Bcl-2/29-90 were calculated from single-site FP assay binding curves shown in Figure 3D and Figures 5B and 5H using Prism software. EC₅₀ values for unlabeled NuBCP-9s binding the same Bcl-2 constructs were derived from single-site FP assay competition curves shown in Figure 3E and Figures 5B and 5H using Prism software. χ^2 values indicate excellent agreement with a single-site binding model. K_i values for unlabeled NuBCP-9s were calculated by the formula $K_i = EC_{50} / [1 + (\text{protein}) / K_d]$ using K_d determined for the FITC-labeled peptides. K_d values were determined from CD binding curves (Figure 4D; Figure 5D) using nonlinear regression analysis for a one-site binding model. Stoichiometry \pm SD was determined as described previously (Jones et al., 2002).

NuBCP-9s Are Capable of Binding to the Loop of Bcl-2

The observation that NuBCP-9 and its enantiomer exhibit similar if not identical effects on Bcl-2 function raised the possibility that their binding interface or interfaces are structurally adaptive. The large regulatory loop of Bcl-2 is predicted to be natively unstructured (Figure S11) and like other loops of this class may be structurally adaptive (Dyson and Wright, 2005; Iakoucheva et al., 2002). Cell-based coimmunoprecipitation (CoIP) (Figure 5A) showed that a Bcl-2 N-terminal fragment containing the BH4 domain and loop, Bcl-2/1-90, interacted with Nur77 mutants (Nur77/DC3, Nur77/DC1, and Nur77/478-504) known to bind Bcl-2. In vitro, NuBCP-9 and its enantiomer bound similarly and competitively to GST-Bcl-2/1-90 as revealed by FP assays (Figure 5B). CD analysis showed that both NuBCP-9s induced similar changes in GST-Bcl-2/1-90 spectra (Figure 5C; Figure S12). The binding affinities of NuBCP-9s for Bcl-2/1-90 ($K_d = 1.7 \mu$ M for NuBCP-9; $K_d = 2.5 \mu$ M for D-NuBCP-9) (Fig-

ure 4E; Figure 5B) are similar to the affinities for Bcl-2 (Figure 4E), as are the stoichiometries (Figures 4D and 4E; Figure 5D). Thus, Bcl-2/1-90 retains the ability of Bcl-2 to bind to NuBCP-9s, excluding the involvement of the hydrophobic groove in Bcl-2, consistent with the inability of a BH3 peptide and ABT-737 to compete with the binding of NuBCP-9 to Bcl-2 (Figure 3E). We next examined whether the Bcl-2 loop alone is capable of binding to NuBCP-9s. The Myc-tagged Bcl-2 loop, Myc-Bcl-2/29-90, interacted with GFP-Nur77/DC3 (Figure 5E). The interaction was inhibited by NuBCP-9 or D-NuBCP-9, but not by NuBCP-9/AA (Figure 5F). Mutations of Thr69 and Ser70 in the loop slightly enhanced its interaction with Nur77/DC3, while insertion of 10 aa in the loop largely impaired the interaction (Figure 5G). Strong support was provided by FP assays showing that both peptides bound to GST-Bcl-2/29-90 protein (Figure 5H). Also, NuBCP-9 and its enantiomer, but not the mutant peptide, competed with FITC-NuBCP-9 for binding to

GST-Bcl-2/29–90. Furthermore, CD analysis showed a similar change of the spectra of GST-Bcl-2/29–90 protein by NuBCP-9 and its enantiomer (Figure 5I; Figure S13). Bcl-2 and Bcl-2/1–90 underwent greater NuBCP-induced changes in their CD spectra than Bcl-2/29–90, suggesting involvement of the BH4 domain. Thus, NuBCP-9 and its enantiomer bind to the Bcl-2 loop.

NuBCP-9 Induces Bcl-2-Dependent Bax Activation

Our observation that NuBCP-9-induced apoptosis is dependent on Bax and/or Bak prompted us to investigate whether and how NuBCP-9 activates Bax. In vitro assays using isolated mitochondria showed that both NuBCP-9 and D-NuBCP-9 induced Bax dimerization, trimerization, and especially oligomerization (Figure 6A) in a concentration-dependent manner (Figure 6B). Such an effect occurred only in the presence of GST-Bcl-2 protein. In DoHH2 lymphoma cells that express high levels of Bcl-2 (Dyer et al., 1996), NuBCP-9s induced Bax dimerization/oligomerization (Figure 6C). Transfection of Bcl-2/1–95 inhibited both NuBCP-9-induced apoptosis (Figure 6D) and Bax activation (Figure 6E). NuBCP-9 also induced Bax activation in H460 cells as revealed by flow cytometric analysis of Bax immunostaining with an anti-Bax antibody (6A7) that recognizes active Bax conformation (Nechushtan et al., 1999) (Figure 6F). Similar to the effect in DoHH2 cells, Bcl-2/1-90 potently inhibited NuBCP-9-induced apoptosis (Figure 6G) and Bax activation in H460 cells (Figure 6H). Furthermore, expression of Bcl-2/ Δ BH3, a Bcl-2 mutant lacking its BH3 domain, inhibited NuBCP-9-induced apoptosis (Figure 6G) and Bax activation (Figure 6H). NuBCP-9-induced Bax activation was observed in wild-type MEFs but not Bcl-2 knockout MEFs (Figure 6I). However, transfection of Bcl-2 into Bcl-2^{-/-} MEFs restored the ability of NuBCP-9 to activate Bax (Figure 6J). Together, these cell-free and cell-based studies demonstrate that NuBCP-9 induces Bax activation in a Bcl-2-dependent manner and that the loop and BH3 regions of Bcl-2 are crucial.

NuBCP-9s Disrupt Bcl-2 Intramolecular Interaction

To study the mechanism by which enantiomeric NuBCPs induce Bcl-2 conformational change, we first examined how the antiapoptotic Bcl-2 conformation was maintained and found that the Bcl-2 BH4 domain could act like a brace to stabilize the C-terminal antiapoptotic BH3-binding pocket. CoIP revealed that a Bcl-2 N-terminal sequence containing the BH4 domain bound a Bcl-2 mutant from which the BH4 domain was removed (Bcl-2/ Δ BH4) (Figure 7A), suggesting an intramolecular interaction between the BH4 domain and the C-terminal region. The BH4 domain could not bind full-length Bcl-2, likely due to inaccessibility of a BH4-binding site in the C-terminal region. However, a strong interaction was observed when Nur77/ Δ DBD or Nur77/DC3 was coexpressed (Figure 7B), suggesting that binding of Nur77 mutants with Bcl-2 reorganizes Bcl-2, leading to the exposure of the BH4-binding site in the C-terminal region. Similarly, addition of NuBCP-9 and its enantiomer induced the binding of the BH4 domain to Bcl-2 (Figure 7C). Removal of the BH4 domain through caspase cleavage of the Bcl-2 loop converts it into a apoptotic molecule (Cheng et al., 1997; Grandgirard et al., 1998). Consistently, a Bcl-2 mutant lacking its BH4 domain was extensively immunostained by anti-Bcl-2 BH3 domain

antibody, while the wild-type Bcl-2 protein was not, indicating that the exposure of the BH3 epitope is blocked directly or indirectly by the BH4 domain (Figure 7D). Thus, our data unravel a mechanism of Bcl-2 conversion in which binding of NuBCP-9 or its enantiomer to the Bcl-2 loop dislodges its BH4 domain, leading to a proapoptotic conformation that exposes the BH3 domain.

NuBCP-9 Disrupts Bcl-2 Interaction with tBid in Liposomes

We next determined how NuBCP-9-induced changes in Bcl-2 conformation result in Bax activation and apoptosis. One way in which Bcl-2 prevents death is by sequestering activator BH3-only family members (such as Bid) and preventing their interaction with Bax/Bak (Cheng et al., 2001; Kuwana et al., 2005; Letai et al., 2002). We recently showed that the interaction between membrane-bound Bcl-2 and tBid results in a conformational alteration in Bcl-2 that induces permeabilization of liposomal membranes to the 0.5 kDa fluorescent dye cascade blue (CB) (Peng et al., 2006). Unlike the interaction of tBid with Bax, the pores in liposomal membranes that result from the interaction of tBid with Bcl-2 are relatively small, allowing the release of CB but not CB-labeled 10 kDa dextran. Although the physiological significance of the tBid-induced Bcl-2 membrane-permeabilizing activity is largely elusive, it offered an opportunity to study the effect of NuBCP-9 on tBid/Bcl-2 interaction in liposomes. When NuBCP-9 was added with Bcl-2 and tBid to liposomes, NuBCP-9, but not NuBCP-9/AA, inhibited the membrane permeabilization induced by tBid/Bcl-2 interaction in a dose-dependent manner (Figure 7E). NuBCP-9 at 1 μ M was sufficient for inhibition, which could not be further increased by using 10 μ M peptide. This result suggests that 10 μ M is a saturating peptide concentration, consistent with our binding studies (Figure 4E). NuBCP-9 alone had no effect on the membrane permeability, even at the highest dose (10 μ M). Thus, NuBCP-9 can inhibit the interaction of Bcl-2 with an activator BH3-only protein, which in turn may activate Bax.

NuBCP-9 Does Not Convert Bcl-2 to a Direct Activator of Bax

Some BH3-only proteins, including Bid and Bim (termed activators), induce Bax/Bak oligomerization through their direct interaction with Bax/Bak (Cheng et al., 2001; Kuwana et al., 2005; Letai et al., 2002). We next tested whether the NuBCP-9-converted Bcl-2 could also function as a direct activator of Bax. As shown in Figure 7F, while adding NuBCP-9 even at a saturating concentration of 10 μ M to 50 nM Bcl-2 induced a marginal but reproducible membrane permeabilization of liposomes, further addition of 50 nM Bax failed to increase the membrane permeability. In contrast, 5 nM tBid strongly induced membrane permeabilization by 50 nM Bax, releasing a cytochrome c surrogate, 10 kDa CB-dextran (Figure 8E). Thus, NuBCP-9 does not induce Bcl-2 to directly activate Bax.

BH3 Peptide from Bcl-2 Reverses Bcl-X_L's Inhibition of tBid-Activated Bax in Liposomes

To study whether NuBCP-9-induced exposure of the BH3 domain in Bcl-2 acts indirectly to induce apoptosis by competing with Bax or Bak for the BH3-binding pockets of antiapoptotic

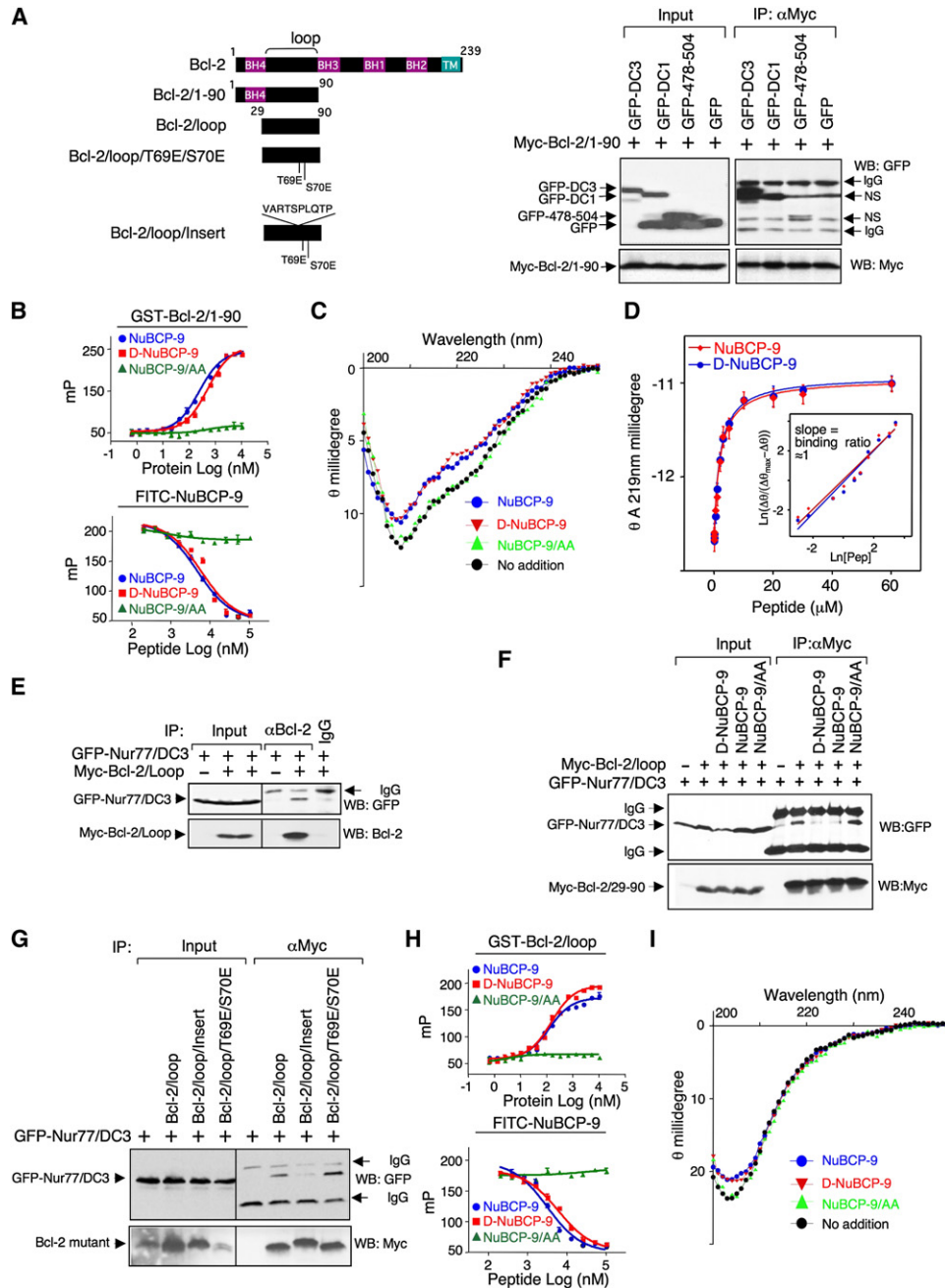


Figure 5. NuBCP-9 and Its Enantiomer Bind to the Loop of Bcl-2

(A) Binding of Bcl-2/1-90 with Nur77 by CoIP. Bcl-2 mutants used are shown in the left panel. The indicated Nur77 mutant expression vector was cotransfected with Bcl-2/1-90 tagged with Myc epitope, and their interaction was analyzed by CoIP using anti-Myc antibody. Specific and nonspecific (NS) bands are indicated. Input represents 5% of cell lysates used for CoIP assays. Data from one of three experiments are shown.

(B) FP assays. Bcl-2/1-90 was incubated with the indicated FITC-NuBCP-r8 (20 nM) in triplicate in PBS (pH 7.6) at 25°C, and FP was determined when the signal stabilized within 20 min. Lower panel: competition experiments were carried out by incubating 200 nM GST-Bcl-2/1-90 protein with 20 nM FITC-NuBCP-r8 in the presence or absence of unlabeled NuBCPs in triplicate, and FP was determined within 20 min upon stabilization of the signal. Data are presented as mean \pm SD.

(C) CD spectra for the binding of NuBCP-9s (30 μ M) to GST-Bcl-2/1-90 (2 μ M) in PBS (pH 7.6) at 25°C. Data from one of three experiments are shown.

(D) Stoichiometry of binding of NuBCP-9 to GST-Bcl-2/1-90. GST-Bcl-2 was titrated with NuBCP-9s in PBS (pH 7.6) at 25°C at 219 nm, where absorption from the free peptide is <0.3% of protein. Stoichiometry was determined as described previously (Jones et al., 2002). Data are presented as mean \pm SD.

(E and F) CoIP assays. HEK293T cells transfected with GFP-Nur77/DC3 and Myc-tagged Bcl-2/29-90 were exposed to NuBCP-9 or D-NuBCP-9, and their interaction was analyzed by CoIP. Input represents 5% of cell lysates used for CoIP assays. Data from one of three experiments are shown.

(G) Mutation or insertion in the loop of Bcl-2 affects loop binding to Nur77. Bcl-2 loop mutants were tagged with Myc epitope and transfected into HEK293T cells with GFP-Nur77/DC3. Cell lysates were prepared and analyzed for interaction of Bcl-2 loop mutants with Nur77/DC3 by CoIP. Input represents 5% of lysates used for CoIP assays. Data from one of three experiments are shown.

(H) Mutation or insertion in the loop of Bcl-2 affects loop binding to Nur77. Bcl-2 loop mutants were tagged with Myc epitope and transfected into HEK293T cells with GFP-Nur77/DC3. Cell lysates were prepared and analyzed for interaction of Bcl-2 loop mutants with Nur77/DC3 by CoIP. Input represents 5% of lysates used for CoIP assays. Data from one of three experiments are shown.

Bcl-2 family members, we mutated two highly conserved BH3 residues (Leu97 and Asp102) in Bcl-2 (Figure 8A) that correspond with residues in the Bak BH3 peptide that are required for displacing BH3 proteins and peptides from the BH3-binding pockets of antiapoptotic Bcl-2 family members (Sattler et al., 1997). The Bcl-2 double mutant (Bcl-2/L97A/D102A) acted dominant negatively, suppressing Nur77 peptide-induced apoptosis (Figure 8B). We then tested whether the Bcl-2 BH3 peptide could directly inhibit Bcl-X_L blocking of tBid-induced Bax permeabilization of liposomes encapsulating the large 10 kDa CB-dextran. As shown in Figure 8C, the inhibitory effect of Bcl-X_L was reversed by Bcl-2 BH3 in a dose-dependent manner, while the mutant BH3 peptide had no effect. Also, the Bcl-2 BH3 peptide alone did not induce Bax-dependent membrane permeabilization, consistent with the observation that the addition of NuBCP-9 to Bcl-2 did not induce Bax-dependent membrane permeability (Figure 7F). Next, we showed using the FP assay that F5M-Cys-labeled Bcl-2 BH3 peptide, but not the double-mutant peptide, bound to GST-Bcl-X_L protein ($K_D = 144.6 \pm 11$ nM) (Figure 8D). Binding of the Bcl-2 BH3 peptide to Bcl-X_L confirmed a previous report (Sattler et al., 1997).

We next determined whether Bcl-2 in the presence of NuBCP-9 could mimic the inhibitory effect of the Bcl-2 BH3 peptide on the activity of Bcl-X_L against tBid-activated Bax. A saturating concentration of NuBCP-9 (10 μ M) was preincubated with Bcl-2 protein to insure full conversion before adding Bcl-X_L. Figure 8E shows that Bcl-X_L inhibition of tBid-induced Bax permeabilization was reversed by NuBCP-9 in a Bcl-2-dependent manner. In contrast, the addition of Bcl-2 to Bcl-X_L further inhibited the tBid-induced Bax activity. Figure 8E also shows that, similar to Bcl-X_L, Bcl-2 alone inhibited the tBid/Bax-mediated membrane permeabilization. Unlike the Bcl-X_L case, the Bcl-2 inhibition was reversed by the addition of NuBCP-9. Together, our liposome results demonstrate that NuBCP-9-induced Bcl-2 conformational change not only neutralizes Bcl-2's inhibition of Bax-mediated membrane permeabilization but also exposes the Bcl-2 BH3 motif, neutralizing Bcl-X_L's inhibition of Bax (Figure 8F).

DISCUSSION

Here we report the identification and characterization of a 9 aa Nur77 Bcl-2-converting peptide, NuBCP-9, which potently induces apoptosis through a pathway that is potentiated by Bcl-2 expression in vitro and in animals (Figure 1; Figure 2; Figures S3 and S4). Bcl-2 is an attractive drug target because its levels are elevated in a majority of human cancers and correlate with the resistance of cancer cells to many chemotherapeutic drugs and γ irradiation. From a therapeutic viewpoint, Bcl-2 overexpression may be advantageous because it distinguishes many cancer cells from normal cells. In this regard, several strategies taking advantage of this difference are currently being in-

vestigated, which may lead to improved cancer treatments. Currently, targeting Bcl-2 has mostly relied on antisense oligonucleotides that inhibit Bcl-2 expression or BH3 peptides and small-molecule surrogates that bind the Bcl-2 BH3-binding pocket, antagonizing its antiapoptotic activity (Bouillet and Strasser, 2002; Degterev et al., 2001; Oltersdorf et al., 2005; Reed, 2002; Walensky et al., 2004). Although it has been known for some time that Bcl-2 can be converted to a proapoptotic form by caspase-3 (Cheng et al., 1997; Grandgirard et al., 1998) or activating proteins including Nur77 (Lin et al., 2004), it has been unclear whether this conversion provides a basis for cancer drug development. NuBCP-9 acts by inducing a Bcl-2 conformational change, raising prospects that NuBCP-9-based drugs and small-molecule Bcl-2 converters might be developed for treating cancers with elevated levels of Bcl-2. The NuBCP-9 enantiomer is protease resistant (Zhou et al., 2002), an important consideration for peptide-based drug development, while short peptides are sometimes forerunners for small-molecule drug development. Our observation that NuBCP-9 and its enantiomer effectively induce tumor regression in animals establishes them as potential therapeutic leads for the treatment of Bcl-2-overexpressing cancers.

Our data demonstrate that NuBCP-9 induces a Bcl-2 conformational change by binding the Bcl-2 loop to dislodge its BH4 domain (Figures 7A–7C), which exposes the BH3 domain (Figure 4; Figure 7D; Figure S7). These results provide further support for the Bcl-2 loop as a regulator of its activity. The Bcl-2 loop is predicted to be natively unstructured (Figure S11). Recent studies have shown that a large unstructured loop can bind different proteins by structural adaptation through coupled folding (Dyson and Wright, 2005). The majority of human cancer-associated and signaling proteins are predicted to have large, natively unstructured loops, which may account for their positions at the center of many biological processes (Dyson and Wright, 2005; Li, 2005; Iakoucheva et al., 2002). The observation that both NuBCP-9 and its enantiomer bind the Bcl-2 loop may be a manifestation of an unstructured, conformationally adaptable loop. The Bcl-2 family of proteins is central to apoptosis. Thus, it is not surprising that the Bcl-2 loop shares many of the characteristics of structurally adaptable regulatory loops, including its large size (69 residues), high proline content (22%), several phosphorylation and caspase cleavage sites, and at least five different protein binding partners (Bruey et al., 2007; Deng et al., 2006; Kang et al., 2005; Lin et al., 2004; Ueno et al., 2000). Consequently, it might be expected that Bcl-2 conversion is subject to multiple levels of regulation, depending on cell type and cellular environment. Of particular interest is that the Bcl-2 loop is enriched by proline residues, which are widely distributed in disordered regulatory loops of proteins from prokaryotes to eukaryotes and display promiscuity and versatility in protein-protein interactions (Li, 2005). Structural analysis of the Bcl-2/NuBCP complex will eventually resolve whether these

(H) FP assays. Upper panel: Bcl-2/29–90 was incubated with the indicated FITC-NuBCP-r8 (20 nM) in triplicate in PBS (pH 7.6) at 25 °C, and FP was determined when the signal stabilized within 20 min. Lower panel: competition experiments were carried out by incubating 200 nM GST-Bcl-2/29–90 protein with 20 nM FITC-NuBCP-r8 in the presence or absence of unlabeled NuBCPs in triplicate, and FP was determined within 20 min upon stabilization of the signal. Data are presented as mean \pm SD.

(I) CD spectra for the binding of NuBCPs (30 μ M) to GST-Bcl-2/29–90 (2 μ M). Data from one of three experiments are shown.

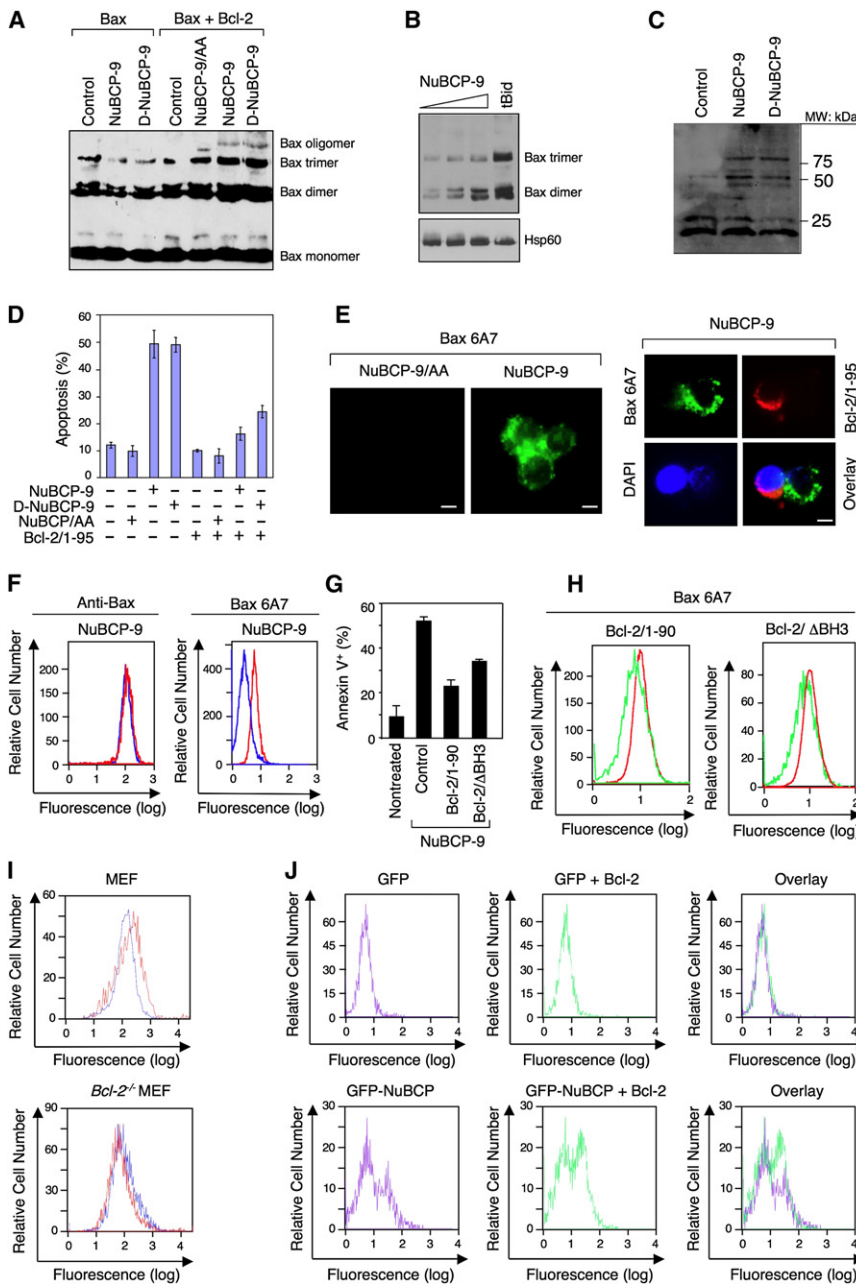


Figure 6. NuBCP-9 Induces Bcl-2-Dependent Bax Activation

(A) Bax dimerization/oligomerization. Isolated mitochondria from HeLa cells were incubated with purified Bax and/or Bcl-2 proteins preincubated with peptide (10 μ M). After crosslinking with bismaleimido-hexane, reactions were analyzed by immunoblotting using anti-Bax antibody (N20). Data from one of five experiments are shown.

(B) Dose-dependent activation of Bax. Isolated mitochondria were incubated with purified Bax and Bcl-2 proteins preincubated with NuBCP-9 (1, 2, and 5 μ M) or tBid protein (100 ng) and analyzed for Bax activation as in (A). Levels of Hsp60 were used as a control. Data from one of three experiments are shown.

(C) Bax dimerization/oligomerization in DoHH2 cells. Cells were treated with the indicated peptide (10 μ M) for 8 hr and analyzed for Bax activation as in (A). Data from one of five experiments are shown.

(D) Inhibition of NuBCP-9-induced apoptosis by Bcl-2/1-95. DoHH2 cells transfected with DsRed-Bcl-2/1-95 or empty vector (pCMV-DsRed, Clontech) were exposed to the indicated peptide (10 μ M) for 12 hr. Transfected cells were assessed for apoptosis by DAPI staining. Bars represent means \pm SD from three experiments.

(E) Inhibition of NuBCP-9-induced Bax activation by Bcl-2/1-95. DoHH2 cells without transfection (left two panels) or transfected with DsRed-Bcl-2/1-95 (right four panels) were exposed to NuBCP-9 or NuBCP-9/AA (10 μ M) as indicated for 12 hr. Cells were then immunostained with anti-Bax antibody (6A7) and analyzed by fluorescence microscopy. About 80% of nontransfected cells exposed to NuBCP-9 showed Bax staining (green) (left panels), while about 50% of DsRed-Bcl-2/1-95-transfected cells (red) failed to display Bax staining (right panels). Scale bars = 10 μ M.

(F) Bax activation in H460 cells. Cells treated with NuBCP-9 (6 μ M) for 16 hr were immunostained with either polyclonal anti-Bax (Invitrogen) or monoclonal 6A7 anti-Bax antibody (Sigma) (Murphy et al., 2000) and anti-rabbit or anti-mouse SRPD-conjugated secondary antibodies. Immunofluorescence was analyzed by flow cytometry. Histograms of peptide-treated cells (red) and untreated cells (blue) are overlaid.

(G) Dominant-negative effect of Bcl-2 mutants. H460 cells in six-well plates were transfected with GFP (0.8 μ g) and empty vector (2 μ g, control) or GFP-Bcl-2/1-90 (2 μ g) or Bcl-2/ Δ BH3 (2 μ g)

alone for 24 hr prior to exposure to NuBCP-9 (6 μ M) for another 10 hr. Apoptosis of transfected cells was determined by annexin V staining. Bars represent means \pm SD from three experiments.

(H) Suppression of Bax activation by Bcl-2 mutants. Bcl-2 mutants were expressed and treated as in (G) and immunostained with anti-Bax antibody (6A7) and SRPD-conjugated secondary antibody. Bax immunofluorescence was analyzed by flow cytometry. Fluorescence of transfected cells (green histogram) is compared to that of nontransfected cells (red histogram) from the same transfection.

(I) NuBCP-9 induces Bax activation in wild-type MEFs but not *Bcl-2*^{-/-} MEFs. Cells were exposed to NuBCP-9 (10 μ M) for 16 hr and immunostained with anti-Bax antibody (6A7) as in (F). Bax immunofluorescence was analyzed by flow cytometry. Histograms of treated (red) and untreated (blue) cells are overlaid. Bax protein levels in MEFs were determined by immunoblotting and did not change with NuBCP-9 treatment.

(J) Expression of Bcl-2 in *Bcl-2*^{-/-} MEFs restores Bax activation by NuBCP. *Bcl-2*^{-/-} MEFs in six-well plates were cotransfected with Bcl-2 (1 μ g) and GFP or GFP-Nur77/478-504 (1 μ g) and immunostained with anti-Bax antibody (6A7). Bax immunofluorescence of GFP- or GFP-Nur77/478-504 (GFP-NuBCP)-expressing cells (purple histogram) is compared to Bcl-2-coexpressing cells (green histogram) by flow cytometry.

proline-rich sequences are responsible for binding to NuBCP-9 and its enantiomer. As many human cancer-associated and signaling proteins contain large, natively disordered regulatory

loops (Dyson and Wright, 2005; Iakoucheva et al., 2002; Li, 2005), proteolytically stable D-peptides may provide a rich source for new drug leads.

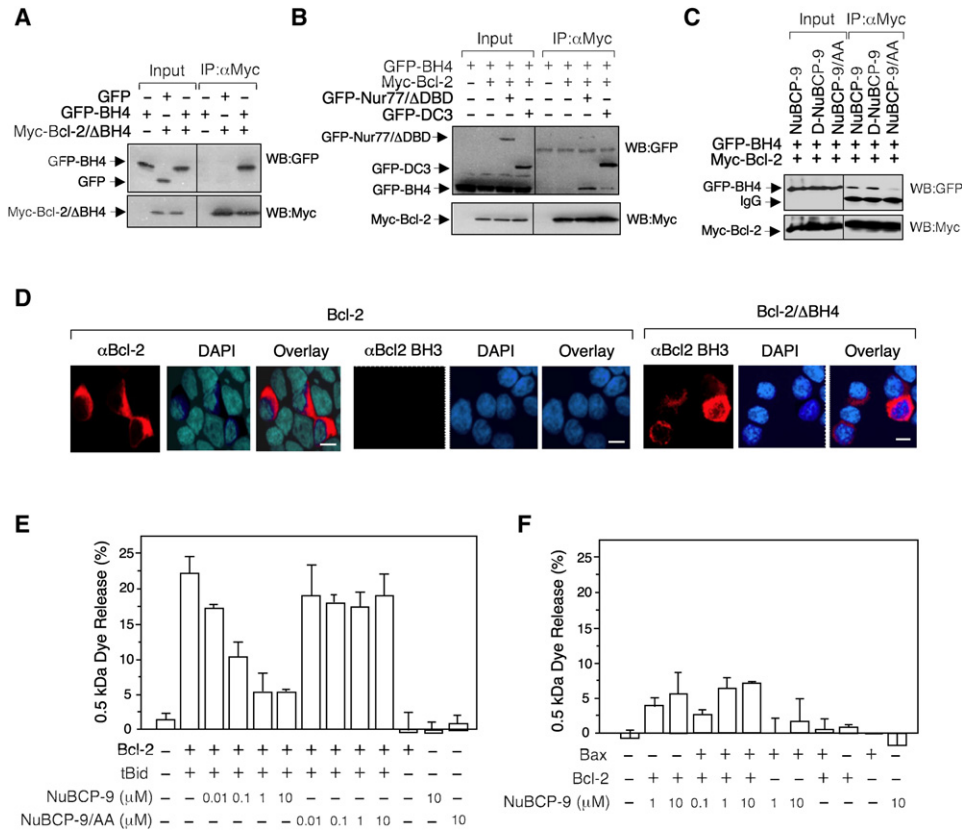


Figure 7. NuBCPs Disrupt Bcl-2's Intramolecular Interaction and Binding with tBid

(A) Intramolecular interaction in Bcl-2. GFP-BH4 or Bcl-2/ΔBH4 was transfected alone or together into HEK293T cells, and their interaction was analyzed by CoIP. (B and C) Nur77 and NuBCP-9s disrupt Bcl-2 intramolecular interaction. The indicated expression vectors were transfected into HEK293T cells. The effect of Nur77/ΔDBD and Nur77/DC3 (B) or NuBCP-9s (C) on the interaction between the BH4 domain and Bcl-2 was analyzed by CoIP. In (A)–(C), input represents 5% of cell lysates used for CoIP assays, and representative data from one of four independent experiments are shown. (D) Removal of the BH4 domain exposes the BH3 domain. HEK293T cells transfected with either Bcl-2 or Bcl-2/ΔBH4 were stained with either anti-Bcl-2 BH3 domain or polyclonal anti-Bcl-2 antibody. Scale bars = 10 μM. (E) NuBCP-9 inhibits tBid/Bcl-2 interaction in liposomes. The membrane permeabilization induced by tBid/Bcl-2 interaction was monitored by the release of 0.5 kDa cascade blue (CB) dye from the liposomes after 3 hr incubation at 37°C. The release resulted in the quenching of CB fluorescence by the anti-CB antibody located outside of the liposomes. The extent of the release was determined by the value of $\Delta F_{\text{protein}}/\Delta F_{\text{titron}}$ as described in Supplemental Data. The effect of NuBCP-9 or NuBCP-9/AA peptide on the release was determined by adding the corresponding peptide at the indicated concentrations to the incubation. Data shown are means of two to four independent experiments, with SD indicated by error bars. (F) NuBCP-9-induced Bcl-2 conversion does not activate Bax in liposomes. The extent of the 0.5 kDa CB dye release by Bax and/or Bcl-2 in the absence or presence of NuBCP-9 peptide was monitored as above. Data shown are means of two to five independent experiments, with SD indicated by error bars.

Induction of apoptosis by NuBCP-9 required expression of either Bax or Bak (Figure 1H) and was associated with their activation (Figure 6). However, the addition of NuBCP-9 to Bcl-2, unlike tBid, did not induce Bax-dependent permeabilization of mitochondrial outer membrane liposomes (Figure 7F), arguing against a direct activation mechanism. Consistent with an indirect activation mechanism, we found that NuBCP-9 inhibited Bcl-2 interaction with tBid (Figure 7E), suggesting that NuBCP-9 may indirectly induce Bax activation by inhibiting Bcl-2 interaction with activator BH3-only proteins. Investigating this further, our liposome data showed that inhibition of tBid-activated Bax by Bcl-2 or Bcl-X_L was reversed by NuBCP-9 (Figure 8E). Our results are reminiscent of previous studies showing that phosphorylation of the unstructured loop prevents Bcl-2 from binding to multidomain proapoptotic members (Bassik et al., 2004) and beclin 1, a BH3-containing autophagic protein (Wei et al.,

2008). Thus, NuBCP-9, similar to BH3 peptides or their small-molecule surrogates, can prevent Bcl-2 from binding and sequestering proapoptotic Bcl-2 family members.

One unique property of NuBCP-9 distinguishing it from Bcl-2 inhibitors is that NuBCP-9 not only antagonizes the survival function of Bcl-2 but also induces a Bcl-2 conformation that inhibits the survival function of its antiapoptotic relatives, such as Bcl-X_L (Figures 8C–8E). Such an effect is likely mediated by its ability to induce exposure of the BH3 domain of Bcl-2 (Figures 4A and 4B; Figure 7D; Figure S7). Mutagenesis of the Bcl-2 BH3 domain demonstrated that it is required for NuBCP-9-induced Bcl-2-dependent apoptosis. Thus, Bcl-2 BH3 mutants act dominant negatively to inhibit NuBCP-9-induced Bcl-2-dependent apoptosis. Consistent with an indirect activation mechanism, we found that NuBCP-9 inhibited Bcl-2 interaction with tBid (Figure 7E), suggesting that NuBCP-9 may indirectly induce Bax activation by inhibiting Bcl-2 interaction with activator BH3-only proteins. Investigating this further, our liposome data showed that inhibition of tBid-activated Bax by Bcl-2 or Bcl-X_L was reversed by NuBCP-9 (Figure 8E). Our results are reminiscent of previous studies showing that phosphorylation of the unstructured loop prevents Bcl-2 from binding to multidomain proapoptotic members (Bassik et al., 2004) and beclin 1, a BH3-containing autophagic protein (Wei et al.,

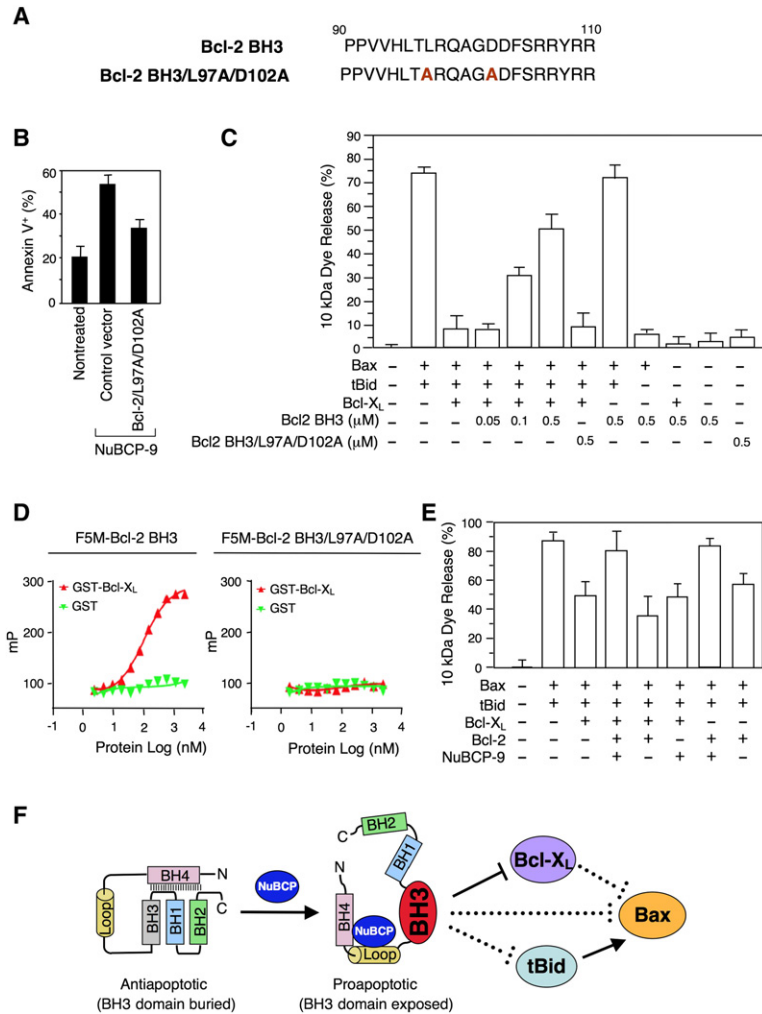


Figure 8. Induction of Apoptosis by the BH3 Domain of Bcl-2

(A) BH3 peptide from Bcl-2 and its mutant. For liposome-based study, peptides only contained the BH3 residues.

(B) Dominant-negative effect of Bcl-2/L97A/D102A. H460 cells in six-well plates were transfected with GFP (1 μg) and empty control vector (2 μg) or GFP (1 μg) and Bcl-2/L97A/D102A (2 μg) for 24 hr prior to exposure to NuBCP-9 (10 μM) for another 16 hr. Apoptosis of transfected cells was determined by annexin V staining. Expression of Bcl-2/L97A/D102A was confirmed by WB (data not shown). Error bars represent mean ± SD.

(C) Bcl-2 BH3 peptide neutralizes the inhibitory effect of Bcl-X_L on tBid-induced Bax membrane-permeabilizing activity in liposomes. The tBid-induced Bax activity was monitored by the release of 10 kDa CB-dextran from the liposomes after 3 hr of incubation at 37°C. The effect of Bcl-X_L and/or Bcl-2 BH3 or its mutant peptide on the tBid/Bax-mediated CB-dextran release was determined by adding the corresponding protein and/or peptide to the incubation at indicated concentrations. Data shown are means of two to three independent experiments, with SD indicated by error bars.

(D) FP assay of binding of Bcl-2 BH3 peptide to Bcl-X_L. The indicated concentration of GST-Bcl-X_L or GST protein was incubated with F5M-Bcl-2 BH3 or F5M-Bcl-2/L97A/D102A (20 nM) in duplicate in modified Dulbecco's PBS (pH 7.4) at 25°C, and FP was determined.

(E) Bcl-2 and NuBCP-9 reverse the inhibitory effect of Bcl-X_L on Bax-dependent membrane permeabilization in liposomes. The effect of Bcl-X_L (10 nM) in the presence of Bcl-2 (200 nM) and/or NuBCP-9 (10 μM) on the tBid (5 nM)/Bax (50 nM)-mediated release of 10 kDa CB-dextran from the liposomes was determined as described in Supplemental Data. Data shown are means of three to five independent experiments, with SD indicated by error bars.

(F) Model of Bcl-2 conversion by NuBCP. Binding of NuBCP to the Bcl-2 loop displaces the BH4 domain, resulting in exposure of the BH3 domain, which leads to either release of proapoptotic BH3-only members (e.g., tBid) from Bcl-2 or inhibition of other antiapoptotic relatives of the Bcl-2 family (e.g., Bcl-X_L) that leads to activation of proapoptotic multi-BH-domain proteins (e.g., Bax).

liposome assays (Figure 8C). Similar to the Bcl-2 BH3 peptide, NuBCP-9-induced exposure of the Bcl-2 BH3 domain also neutralized the inhibitory effect of Bcl-X_L on Bax activation (Figure 8E). Thus, NuBCP-9 is distinguished from Bcl-2 inhibitors in that it also converts Bcl-2 into a "BH3-like" molecule that in turn inhibits its antiapoptotic relative Bcl-X_L.

EXPERIMENTAL PROCEDURES

Peptide Synthesis

Peptides were synthesized as described in Supplemental Experimental Procedures.

Fluorescence Polarization Assays

GST-Bcl-2, GST-Bcl-X_L, or GST protein was incubated briefly with FITC- or F5M-conjugated peptide with or without competitors in Greiner Fluotrac 600 96-well microplates. Fluorescence polarization was recorded using an Analyst HT 96-384 microplate reader (Molecular Devices) with excitation wavelength set at 485 nm and dynamic polarizer for emission at 530 nm.

Circular Dichroism Spectroscopy

CD spectra were determined as described in Supplemental Experimental Procedures.

Apoptosis Assays

Nuclear morphological change analysis and flow cytometric analysis of annexin V binding were performed as described previously (Li et al., 2000; Lin et al., 2004). For determination of DNA fragmentation in tumor tissue, TUNEL assay was used. Peptide treatments were performed in medium with 10% FBS unless otherwise specified.

Immunoblotting and CoIP Assays

For CoIP assay, HEK293T cells transfected with various expression vectors were incubated with the appropriate antibodies, and immunoprecipitates were analyzed by immunoblotting as described previously (Li et al., 2000; Lin et al., 2004). For all cell-based experiments, peptides fused with a cell-penetrating-peptide (r8) were used unless otherwise stated.

Mitochondria Purification

Mitochondria were prepared from HeLa cells as described previously (Zhai et al., 2005).

Bax Activation Assays

Cell-based and in vitro Bax activation assays were performed as described in Supplemental Experimental Procedures.

Liposome Assays

Liposomes of mitochondrial outer membrane lipid composition with cascade blue (CB) or CB-labeled 10 kDa encapsulated dextran were prepared by the

extrusion method (Peng et al., 2006; Tan et al., 2006) and used for assaying Bcl-2 interactions with tBid, Bax, Bcl-X_L, and NuBCP-9 as described in Supplemental Experimental Procedures.

Clonogenic Survival Assays

Clonogenic survival assays were performed as described in Supplemental Experimental Procedures.

Animal Studies

Female SCID mice (6 weeks old, Taconic) were injected with 10⁶ MDA-MB435 cells. Tumors were palpable on day 7. On days 10 and 13, peptides (620 μg in 50 μl PBS) were injected into the tumor areas of five mice. Tumor volumes (length² × width/2) were determined using calipers. No weight changes were observed. Established tumors in mice were injected with peptides, and tumor tissues were excised and sectioned after 3 days. Tissues were fixed in 10% buffered formalin and then rapidly paraffin-embedded. Apoptosis was detected by TUNEL assay. All procedures were performed according to protocols approved by the Institutional Animal Care and Use Committee of the Burnham Institute.

SUPPLEMENTAL DATA

The Supplemental Data include Supplemental Experimental Procedures, Supplemental References, and thirteen figures and can be found with this article online at <http://www.cancercell.org/cgi/content/full/14/4/285/DC1/>.

ACKNOWLEDGMENTS

We thank S. Korsmeyer, S. Lowe, and S. Weintraub for knockout MEFs; K. Webster, D. Koch, J. Peng, D. King, R. Newlin, J. Meerloo, L. Wang, E. Monosov, N. Marshall, and Z. Zhang for technical assistance; D. Andrews for comments; and L. Frazer for preparation of the manuscript. This work was supported in part by grants to X.-k.Z., J.C.R., A.C.S., and J.L. from the National Institutes of Health (CA109345, CA119785, GM060554, and GM062964), the US Army Medical Research and Materiel Command (W81XWH-08-1-0478 and DAMD17-03-1-0427), the California Tobacco-Related Diseases Research Program (CTRDRP) (11RT-0081), the California Breast Cancer Research Program (12IB-0168), the Susan G. Komen Breast Cancer Foundation (BCTR043351), and the 985 Project of Xiamen University. S.K.K. was supported by a new investigator award from CTRDRP and the Linus Pauling Institute at the Oregon State University.

Received: December 3, 2007

Revised: August 29, 2008

Accepted: September 8, 2008

Published: October 6, 2008

REFERENCES

Bassik, M.C., Scorrano, L., Oakes, S.A., Pozzan, T., and Korsmeyer, S.J. (2004). Phosphorylation of BCL-2 regulates ER Ca²⁺ homeostasis and apoptosis. *EMBO J.* 23, 1207–1216.

Blagosklonny, M.V. (2001). Unwinding the loop of Bcl-2 phosphorylation. *Leukemia* 15, 869–874.

Bouillet, P., and Strasser, A. (2002). BH3-only proteins - evolutionarily conserved proapoptotic Bcl-2 family members essential for initiating programmed cell death. *J. Cell Sci.* 115, 1567–1574.

Bruey, J.M., Bruey-Sedano, N., Luciano, F., Zhai, D., Balpai, R., Xu, C., Kress, C.L., Bailly-Maitre, B., Li, X., Osterman, A., et al. (2007). Bcl-2 and Bcl-X_L regulate proinflammatory caspase-1 activation by interaction with NALP1. *Cell* 129, 45–56.

Cheng, E.H., Kirsch, D.G., Clem, R.J., Ravi, R., Kastan, M.B., Bedi, A., Ueno, K., and Hardwick, J.M. (1997). Conversion of Bcl-2 to a Bax-like death effector by caspases. *Science* 278, 1966–1968.

Cheng, E.H., Wei, M.C., Weiler, S., Flavell, R.A., Mak, T.W., Lindsten, T., and Korsmeyer, S.J. (2001). BCL-2, BCL-X(L) sequester BH3 domain-only mole-

cules preventing BAX- and BAK-mediated mitochondrial apoptosis. *Mol. Cell* 8, 705–711.

Chipuk, J.E., Bouchier-Hayes, L., Kuwana, T., Newmeyer, D.D., and Green, D.R. (2005). PUMA couples the nuclear and cytoplasmic proapoptotic function of p53. *Science* 309, 1732–1735.

Colussi, P.A., Quinn, L.M., Huang, D.C., Coombe, M., Read, S.H., Richardson, H., and Kumar, S. (2000). Debcl, a proapoptotic Bcl-2 homologue, is a component of the *Drosophila melanogaster* cell death machinery. *J. Cell Biol.* 148, 703–714.

Cory, S., Huang, D.C., and Adams, J.M. (2003). The Bcl-2 family: roles in cell survival and oncogenesis. *Oncogene* 22, 8590–8607.

Degterev, A., Lugovskoy, A., Cardone, M., Mulley, B., Wagner, G., Mitchison, T., and Yuan, J. (2001). Identification of small-molecule inhibitors of interaction between the BH3 domain and Bcl-x_L. *Nat. Cell Biol.* 3, 173–182.

Deng, X., Gao, F., Flagg, T., Anderson, J., and May, W.S. (2006). Bcl2's flexible loop domain regulates p53 binding and survival. *Mol. Cell Biol.* 26, 4421–4434.

Dyer, M.J., Lillington, D.M., Bastard, C., Tilly, H., Lens, D., Heward, J.M., Stranks, G., Morilla, R., Monrad, S., Guglielmi, P., et al. (1996). Concurrent activation of MYC and BCL2 in B cell non-Hodgkin lymphoma cell lines by translocation of both oncogenes to the same immunoglobulin heavy chain locus. *Leukemia* 10, 1198–1208.

Dyson, H.J., and Wright, P.E. (2005). Intrinsically unstructured proteins and their functions. *Nat. Rev. Mol. Cell Biol.* 6, 197–208.

Grandgirard, D., Studer, E., Monney, L., Belser, T., Fellay, I., Borner, C., and Michel, M.R. (1998). Alphaviruses induce apoptosis in Bcl-2-overexpressing cells: evidence for a caspase-mediated, proteolytic inactivation of Bcl-2. *EMBO J.* 17, 1268–1278.

Green, D.R., and Kroemer, G. (2004). The pathophysiology of mitochondrial cell death. *Science* 305, 626–629.

Iakoucheva, L.M., Brown, C.J., Lawson, J.D., Obradovic, Z., and Dunker, A.K. (2002). Intrinsic disorder in cell-signaling and cancer-associated proteins. *J. Mol. Biol.* 323, 573–584.

Igaki, T., Kanuka, H., Inohara, N., Sawamoto, K., Nunez, G., Okano, H., and Miura, M. (2000). Drob-1, a *Drosophila* member of the Bcl-2/CED-9 family that promotes cell death. *Proc. Natl. Acad. Sci. USA* 97, 662–667.

Jones, G., Zhou, X., and Lu, L.N. (2002). Inclusion by beta-cyclodextrin of a pyrene-labeled dipeptide photoprobe. *Tetrahedron Lett.* 43, 6079–6082.

Jones, S.W., Christison, R., Bundell, K., Voyce, C.J., Brockbank, S.M., Newham, P., and Lindsay, M.A. (2005). Characterisation of cell-penetrating peptide-mediated peptide delivery. *Br. J. Pharmacol.* 145, 1093–1102.

Kang, C.B., Tai, J., Chia, J., and Yoon, H.S. (2005). The flexible loop of Bcl-2 is required for molecular interaction with immunosuppressant FK-506 binding protein 38 (FKBP38). *FEBS Lett.* 579, 1469–1476.

Kuwana, T., Bouchier-Hayes, L., Chipuk, J.E., Bonzon, C., Sullivan, B.A., Green, D.R., and Newmeyer, D.D. (2005). BH3 domains of BH3-only proteins differentially regulate Bax-mediated mitochondrial membrane permeabilization both directly and indirectly. *Mol. Cell* 17, 525–535.

Leber, B., Lin, J., and Andrews, D.W. (2007). Embedded together: the life and death consequences of interaction of the Bcl-2 family with membranes. *Apoptosis* 12, 897–911.

Letai, A., Bassik, M.C., Walensky, L.D., Sorcinelli, M.D., Weiler, S., and Korsmeyer, S.J. (2002). Distinct BH3 domains either sensitize or activate mitochondrial apoptosis, serving as prototype cancer therapeutics. *Cancer Cell* 2, 183–192.

Leu, J.I., Dumont, P., Hafey, M., Murphy, M.E., and George, D.L. (2004). Mitochondrial p53 activates Bak and causes disruption of a Bak-Mcl1 complex. *Nat. Cell Biol.* 6, 443–450.

Li, H., Kolluri, S.K., Gu, J., Dawson, M.I., Cao, X., Hobbs, P.D., Lin, B., Chen, G., Lu, J., Lin, F., et al. (2000). Cytochrome c release and apoptosis induced by mitochondrial targeting of nuclear orphan receptor TR3. *Science* 289, 1159–1164.

Li, S.S. (2005). Specificity and versatility of SH3 and other proline-recognition domains: structural basis and implications for cellular signal transduction. *Biochem. J.* 390, 641–653.

- Lin, B., Kolluri, S.K., Lin, F., Liu, W., Han, Y.H., Cao, X., Dawson, M.I., Reed, J.C., and Zhang, X.K. (2004). Conversion of Bcl-2 from protector to killer by interaction with nuclear orphan receptor Nur77/TR3. *Cell* 116, 527–540.
- Luciano, F., Krajewska, M., Ortiz-Rubio, P., Krajewski, S., Zhai, D., Faustin, B., Bruey, J.M., Bailly-Maitre, B., Lichtenstein, A., Kolluri, S.K., et al. (2007). Nur77 converts phenotype of Bcl-2, an antiapoptotic protein expressed in plasma cells and myeloma. *Blood* 109, 3849–3855.
- Mihara, M., Erster, S., Zaika, A., Petrenko, O., Chittenden, T., Pancoska, P., and Moll, U.M. (2003). p53 has a direct apoptogenic role at the mitochondria. *Mol. Cell* 11, 577–590.
- Moll, U.M., Marchenko, N., and Zhang, X.K. (2006). p53 and Nur77/TR3 - transcription factors that directly target mitochondria for cell death induction. *Oncogene* 25, 4725–4743.
- Murphy, K.M., Streips, U.N., and Lock, R.B. (2000). Bcl-2 inhibits a Fas-induced conformational change in the Bax N terminus and Bax mitochondrial translocation. *J. Biol. Chem.* 275, 17225–17228.
- Nechushtan, A., Smith, C.L., Hsu, Y.T., and Youle, R.J. (1999). Conformation of the Bax C-terminus regulates subcellular location and cell death. *EMBO J.* 18, 2330–2341.
- Oltersdorf, T., Elmore, S.W., Shoemaker, A.R., Armstrong, R.C., Augeri, D.J., Belli, B.A., Bruncko, M., Deckwerth, T.L., Dinges, J., Hajduk, P.J., et al. (2005). An inhibitor of Bcl-2 family proteins induces regression of solid tumours. *Nature* 435, 677–681.
- Peng, J., Tan, C., Roberts, G.J., Nikolaeva, O., Zhang, Z., Lapolla, S.M., Primorac, S., Andrews, D.W., and Lin, J. (2006). tBid elicits a conformational alteration in membrane-bound Bcl-2 such that it inhibits Bax pore formation. *J. Biol. Chem.* 281, 35802–35811.
- Ramaswamy, S., Ross, K.N., Lander, E.S., and Golub, T.R. (2003). A molecular signature of metastasis in primary solid tumors. *Nat. Genet.* 33, 49–54.
- Reed, J.C. (1998). Bcl-2 family proteins. *Oncogene* 17, 3225–3236.
- Reed, J.C. (2002). Apoptosis-based therapies. *Nat. Rev. Drug Discov.* 1, 111–121.
- Sattler, M., Liang, H., Nettlesheim, D., Meadows, R.P., Harlan, J.E., Eberstadt, M., Yoon, H.S., Shuker, S.B., Chang, B.S., Minn, A.J., et al. (1997). Structure of Bcl-xL-Bak peptide complex: recognition between regulators of apoptosis. *Science* 275, 983–986.
- Shipp, M.A., Ross, K.N., Tamayo, P., Weng, A.P., Kutok, J.L., Aguiar, R.C., Gaasenbeek, M., Angelo, M., Reich, M., Pinkus, G.S., et al. (2002). Diffuse large B-cell lymphoma outcome prediction by gene-expression profiling and supervised machine learning. *Nat. Med.* 8, 68–74.
- Tan, C., Dlugosz, P.J., Peng, J., Zhang, Z., Lapolla, S.M., Plafker, S.M., Andrews, D.W., and Lin, J. (2006). Auto-activation of the apoptosis protein Bax increases mitochondrial membrane permeability and is inhibited by Bcl-2. *J. Biol. Chem.* 281, 14764–14775.
- Thompson, J., and Winoto, A. (2008). During negative selection, Nur77 family proteins translocate to mitochondria where they associate with Bcl-2 and expose its proapoptotic BH3 domain. *J. Exp. Med.* 205, 1029–1036.
- Ueno, H., Kondo, E., Yamamoto-Honda, R., Tobe, K., Nakamoto, T., Sasaki, K., Mitani, K., Furusaka, A., Tanaka, T., Tsujimoto, Y., et al. (2000). Association of insulin receptor substrate proteins with Bcl-2 and their effects on its phosphorylation and antiapoptotic function. *Mol. Biol. Cell* 11, 735–746.
- Vander Heiden, M.G., and Thompson, C.B. (1999). Bcl-2 proteins: regulators of apoptosis or of mitochondrial homeostasis? *Nat. Cell Biol.* 1, E209–E216.
- Walensky, L.D., Kung, A.L., Escher, I., Malia, T.J., Barbuto, S., Wright, R.D., Wagner, G., Verdine, G.L., and Korsmeyer, S.J. (2004). Activation of apoptosis in vivo by a hydrocarbon-stapled BH3 helix. *Science* 305, 1466–1470.
- Wei, Y., Pattingre, S., Sinha, S., Bassik, M., and Levine, B. (2008). JNK1-mediated phosphorylation of Bcl-2 regulates starvation-induced autophagy. *Mol. Cell* 30, 678–688.
- Willis, S.N., and Adams, J.M. (2005). Life in the balance: how BH3-only proteins induce apoptosis. *Curr. Opin. Cell Biol.* 17, 617–625.
- Willis, S.N., Fletcher, J.I., Kaufmann, T., van Delft, M.F., Chen, L., Czabotar, P.E., Ierino, H., Lee, E.F., Fairlie, W.D., Bouillet, P., et al. (2007). Apoptosis initiated when BH3 ligands engage multiple Bcl-2 homologs, not Bax or Bak. *Science* 315, 856–859.
- Xue, D., and Horvitz, H.R. (1997). *Caenorhabditis elegans* CED-9 protein is a bifunctional cell-death inhibitor. *Nature* 390, 305–308.
- Zhai, D., Luciano, F., Zhu, X., Guo, B., Satterthwait, A.C., and Reed, J.C. (2005). Humanin binds and nullifies Bid activity by blocking its activation of Bax and Bak. *J. Biol. Chem.* 280, 15815–15824.
- Zhang, X.K. (2007). Targeting Nur77 translocation. *Expert Opin. Ther. Targets* 11, 69–79.
- Zhou, N., Luo, Z., Luo, J., Fan, X., Cayabyab, M., Hiraoka, M., Liu, D., Han, X., Pesavento, J., Dong, C.Z., et al. (2002). Exploring the stereochemistry of CXCR4-peptide recognition and inhibiting HIV-1 entry with D-peptides derived from chemokines. *J. Biol. Chem.* 277, 17476–17485.

Supplemental Data

Article

A Short Nur77-Derived Peptide Converts Bcl-2

from a Protector to a Killer

Siva Kumar Kolluri, Xiuwen Zhu, Xin Zhou, Bingzhen Lin, Ya Chen, Kai Sun, Xuefei Tian, James Town, Xihua Cao, Feng Lin, Dayong Zhai, Shinichi Kitada, Frederick Luciano, Edmond O'Donnell, Yu Cao, Feng He, Jialing Lin, John C. Reed, Arnold C. Satterthwait, and Xiao-kun Zhang

Supplemental Experimental Procedures

Peptide Synthesis

Peptides were synthesized on MBHA resin using Fmoc synthesis and DIC/HOBt coupling with an Advanced Chem Tech 350 and 396 multiple peptide synthesizer. All peptides except FITC-peptides were acetylated on their N-termini and all were amidated on their C-termini. Standard deprotection conditions were used for all peptides except those with Pbf-protected D-arginine octamers, which were treated for 6 hr. Peptides were purified by HPLC on C18 columns and confirmed by MALDI mass analysis. Disulfide linked peptides were prepared as described (Giriat and Muir, 2003). Peptides with C-terminal cysteines were covalently linked to chloroacetylated N-aminocaproic acid in a displacement reaction.

CD Spectroscopy

Stock solutions of 3 mM peptide in 30% acetonitrile/water were added to 0.5 ml of 2 μ M purified GST-proteins in PBS, pH 7.6. CD spectra were obtained in a 0.2 cm path length cell at 20°C using an AVIV 62 DS spectropolarimeter for a wavelength range from 200 to 260 nm with a step size of 1nm averaged for 5 sec. Three spectra were corrected for background and averaged for each sample. The Kd was determined using nonlinear regression analysis for a one-site-binding model ($\chi^2 > 0.98$).

Apoptosis Assays and Peptide Treatments

Nuclear morphological change analysis, cells were trypsinized, washed with PBS, fixed with 3.7% paraformaldehyde, and stained with DAPI (4,6-diamidino-2-phenylindole) (1 μ g/ml) to visualize the nuclei by fluorescent microscopy. Apoptosis was also measured by annexin V binding followed by flow cytometry. For the determination of DNA fragmentation in tumor tissue, the TUNEL assay was used.

Clonogenic Survival Assay

Cells were seeded in 24 well plates at a density of 150 cells/well. Cells were allowed to grow for 36 hours, at which time media was removed and replaced with fresh media containing NuBCP-9, D-NuBCP-9-pen, or NuBCP-9/AA-pen (Control). After 48 hours of treatment, the peptide-

containing media was removed and replaced with fresh media. Cells were allowed to grow until colonies had reached a desirable density as determined by checking non-treated wells (approximately 6 days), at which time they were fixed and stained. Typically each colony counted contained more than 50 cells.

Mitochondria Purification

HeLa cells were pelleted by centrifugation and then washed once in HM buffer (10 mM HEPES, pH 7.4, 250 mM mannitol, 10 mM KCl, 5 mM MgCl₂, 1 mM EGTA), containing 1 mM phenylmethylsulfonyl fluoride and a mixture of protease inhibitors (Roche Applied Science). The cell pellet was then homogenized in HM buffer by 50 strokes of a Dounce homogenizer, using a B-type pestle. The homogenate was centrifuged twice at 600 x g for 5 min to remove nuclei and debris. The resulting supernatant was centrifuged at 10,000 x g for 10 min, and the resulting mitochondria-containing pellet was washed twice with the HM buffer.

Bax Activation Assays

For in vitro Bax activation assay, 10 µl of mitochondria (50 µg) was added into a final volume of 50 µl of HM buffer containing purified Bax or GST-Bcl-2 protein preincubated with Nur77 peptide at 30°C for 1 hr. Oligomerization of Bax was assessed by chemical cross-linking. In brief, dimethyl sulfoxide or bismaleimido-hexane (BMH) cross-linker (Pierce) dissolved in dimethyl sulfoxide was added to mitochondria at a final concentration of 5 µM for 30 min at 30°C. The reactions were quenched with 50 mM cysteine for 15 min at room temperature. Mitochondria were then analyzed by SDS-PAGE/immunoblotting using anti-Bax antibody (N20) (Santa Cruz). For cell-based Bax activation, cells lysates were prepared and incubated with 5 µM BMH for 2 hr at 4°C. Subcellular fractionation was performed to obtain the HM pellets, which were lysed in 1% CHAPS buffer for immunoblotting. For immunostaining, cells were fixed in 4% paraformaldehyde, permeabilized with 0.1% triton X-100, and stained with Bax/d21 antibody (1:300) or Bax (6A7) antibody (1:500) followed by Cy3-conjugated anti-rabbit IgG or Cy3-conjugated anti-mouse IgG, respectively.

Liposome Assays

Liposomes of mitochondrial outer membrane (MOM) lipid composition and with Cascade Blue (CB; MW=0.5 kDa) or CB-dextran (MW=10 kDa) encapsulated were prepared by the extrusion method as described (Tan et al., 2006). To facilitate binding of His₆-tagged Bcl-2 to membranes, a Ni²⁺-chelating lipid analog was incorporated in the liposomes as described (Peng et al., 2006). CB or CB-dextran release from liposomes was assayed by fluorescence quenching. Briefly, liposomes made by 12.5 µM lipids with CB dyes or CB-dextran encapsulated were mixed with 6 µg/ml anti-CB antibodies, and after the initial emission intensity (F_0) was taken, 50 nM His₆-Bcl-2 (Zhang et al., 2004), 50 nM GST-Bcl-X_L, 5 nM tBid, 50 nM Bax (Yethon et al., 2003), and/or NuBCP or Bcl-2 BH3 peptides were added. The fluorescence intensity (F) was then measured after a 3 hr incubation at 37°C. At the end of the experiment 0.1% Triton X-100 was added and the final intensity (F_t) was measured. The extent of CB or CB-dextran release is proportional to the extent of fluorescence quenching that is equal to $\Delta F_{\text{Protein}}/\Delta F_{\text{Triton}}$, where $\Delta F_{\text{Protein}} = F_0 - F$, and $\Delta F_{\text{Triton}} = F_0 - F_t$. All fluorescence intensities were measured using SLM-8100 spectrofluorometer as described (Peng et al., 2006).

To test whether NuBCP-9 converts Bcl-2 to an inhibitor that neutralizes the inhibitory effect of Bcl-X_L on tBid-activated Bax, appropriate volumes of NuBCP (1 mM) and Bcl-2 (72

μM) stock solutions were pre-incubated on ice for 5 min, then mixed with Bcl-X_L stock solution (1.6 μM) and kept on ice for 20 min. After adding liposome (1.6 mM) and anti-CB antibody (3 mg/ml) stock solutions and incubating on ice for 10 min, 240 μL of buffer A (Tan et al., 2006) was added to bring the final concentration of NuBCP to 10 μM , Bcl-2 200 nM, Bcl-X_L 10 nM, liposome 12.5 μM , and anti-CB antibody 6 $\mu\text{g}/\text{mL}$. The sample was then incubated at 37°C for 2 min and F₀ measured. After adding Bax and tBid to 50 nM and 5 nM, respectively, the sample was incubated at 37°C for 3 hr, before F and F_t were measured as described above.

Supplemental References

- Giriati, I., and Muir, T. W. (2003). Protein semi-synthesis in living cells. *J Am Chem Soc* 125, 7180-7181.
- Li, H., Kolluri, S. K., Gu, J., Dawson, M. I., Cao, X., Hobbs, P. D., Lin, B., Chen, G., Lu, J., Lin, F., *et al.* (2000). Cytochrome c release and apoptosis induced by mitochondrial targeting of nuclear orphan receptor TR3 [see comments] [comment]. *Science* 289, 1159-1164.
- Li, X., Romero, P., Rani, M., Dunker, A. K., and Obradovic, Z. (1999). Predicting protein disorder for N-, C-, and internal regions. *Genome Informatics* 10, 30-40.
- Lin, B., Kolluri, S. K., Lin, F., Liu, W., Han, Y. H., Cao, X., Dawson, M. I., Reed, J. C., and Zhang, X. K. (2004). Conversion of Bcl-2 from protector to killer by interaction with nuclear orphan receptor Nur77/TR3. *Cell* 116, 527-540.
- Peng, J., Tan, C., Roberts, G. J., Nikolaeva, O., Zhang, Z., Lapolla, S. M., Primorac, S., Andrews, D. W., and Lin, J. (2006). tBid elicits a conformational alteration in membrane-bound Bcl-2 such that it inhibits Bax pore formation. *J. Biol. Chem.* 281, 35802-35811.
- Romero, P., Obradovic, Z., and Dunker, A.K. (1997). Sequence data analysis for long disordered regions prediction in the calcineurin family. *Genome Informatics* 8,110-124.
- Romero, P., Obradovic, Z. Li, X. Garner, E., Brown, C., and Dunker, A. K. (2001). Sequence complexity of disordered protein. *Proteins: Struct. Funct. Gen.* 42, 38-48.
- Tan, C., Dlugosz, P. J., Peng, J., Zhang, Z., Lapolla, S. M., Plafker, S. M., Andrews, D. W., and Lin, J. (2006). Auto-activation of the apoptosis protein Bax increases mitochondrial membrane permeability and is inhibited by Bcl-2. *J. Biol. Chem.* 281, 14764-14775.
- Yethon, J. A., Epand, R. F., Leber, B., Epand, R. M., and Andrews, D. W. (2004). Interaction with a membrane surface triggers a reversible conformational change in Bax normally associated with induction of apoptosis. *J. Biol. Chem.* 278, 48935-48941.
- Zhai, D., Luciano, F., Zhu, X., Guo, B., Satterthwait, A. C., and Reed, J. C. (2005). Humanin binds and nullifies Bid activity by blocking its activation of Bax and Bak. *J. Biol. Chem.* 280, 15815-15824.
- Zhang, Z., Lapolla, S.M., Annis, M.G., Truscott, M., Roberts, G.J., Miao, Y., Shao, Y., Tan, C., Peng, J., Johnson, A.E., Zhang, X.C., Andrews, D.W., and Lin, J. (2004). Bcl-2 homodimerization involves two distinct binding surfaces, a topographic arrangement that provides an effective mechanism for Bcl-2 to capture activated Bax. *J. Biol. Chem.* 279, 43920-43928.

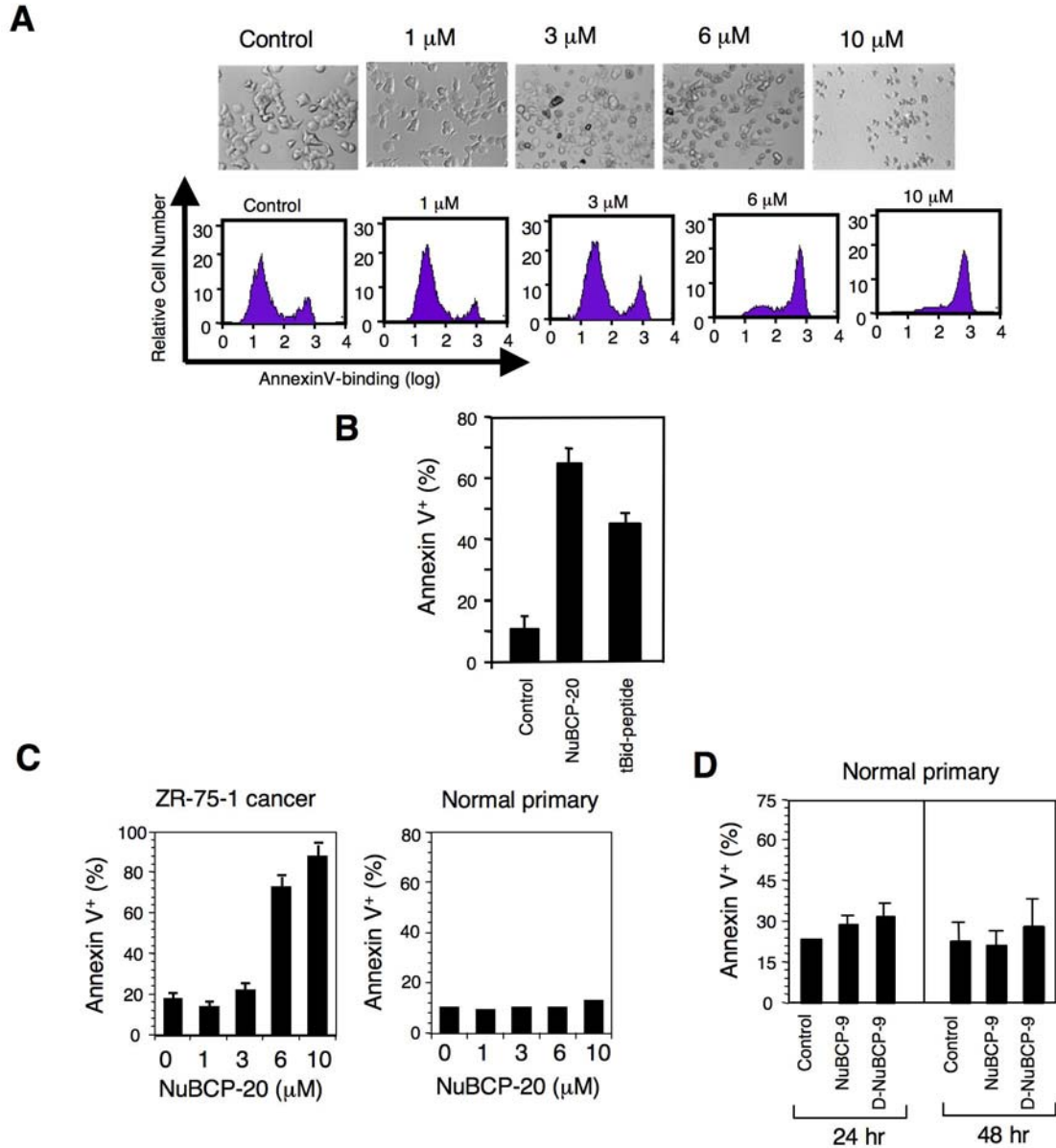


Figure S1. Growth Inhibition and Apoptosis Induction by NuBCP

(A) Growth inhibition and apoptosis induction by NuBCP. ZR-75-1 breast cancer cells were exposed to the indicated concentrations of NuBCP-20-r8 peptide for 16 hr and growth inhibition was visualized by microscopy (upper panel). Apoptosis was determined by annexin V staining (Bottom panel).

(B) Apoptosis induction by NuBCP-20-r8 and t-Bid BH3 peptide-r8. ZR-75-1 cells were exposed to 20 μ M of NuBCP-20-r8 or t-Bid BH3 peptide for 16 hr. Apoptosis was determined by annexin V staining.

(C and D) NuBCPs induce apoptosis in ZR-75-1 breast cancer but not in normal primary mammary epithelial cells. Cells were seeded at 60% confluency and then exposed to NuBCP-20-r8 for 16 hr (C), or L- or D-NuBCP-9-r8 for 24 hr or 48 hr (D). Apoptosis was determined by annexin V staining. The bars represent means \pm SD from three independent experiments.

Results: These studies demonstrate that NuBCPs are very potent inducers of apoptosis of cancer cells, even more effective than t-bid peptide (an effective apoptotic BH3-peptide). Moreover, our results show that normal primary mammary epithelial cells are resistant to NuBCPs. Such a resistance was observed over a range of incubation times (24 hr and 48 hr).

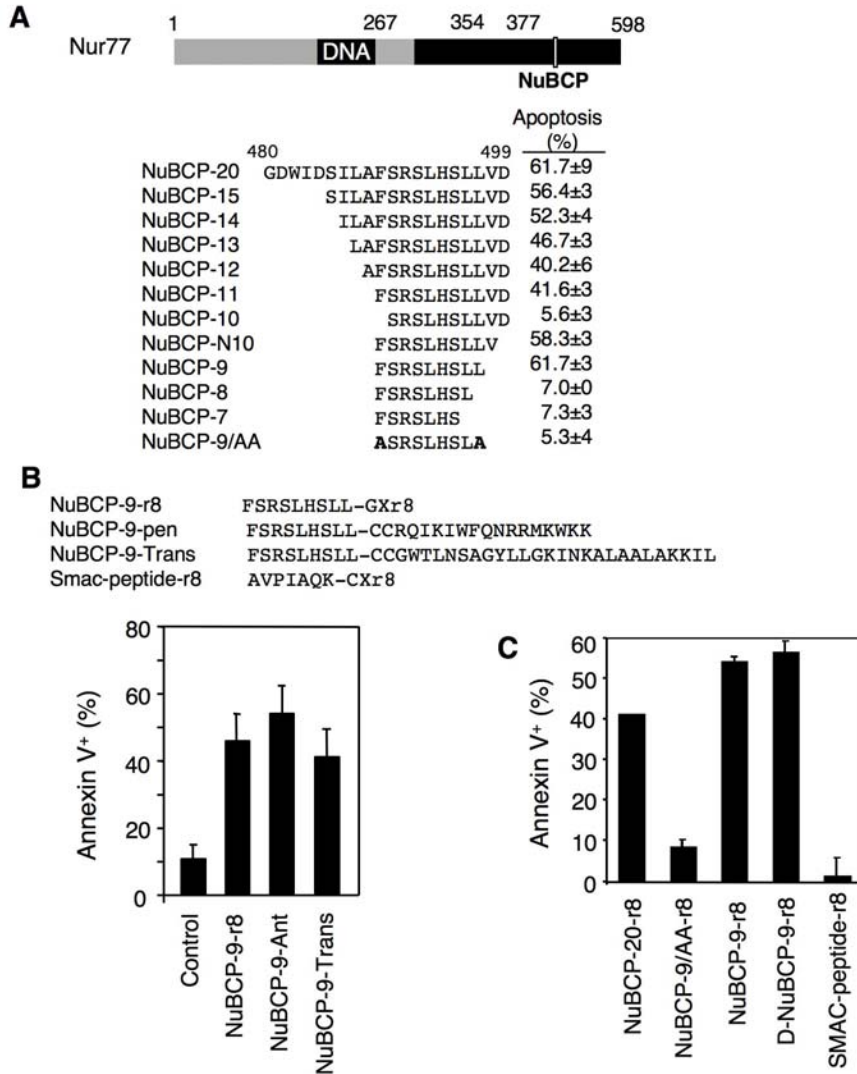


Figure S2.

(A) Serial deletion analysis of NuBCP-20. Apoptotic effect of peptides conjugated with polyarginine (10 μ M) in H460 cells.

(B) Characterization of NuBCP-9 fused with different cell penetrating peptides (CCPs), penetratin (Ant) and transportan-10 (Trans). Apoptotic effect of NuBCP-9 conjugated with CPPs (10 μ M) was determined by annexin V staining in H460 cells. X, N-aminocaproic acid; CX, covalent linkage between cysteine thiol and acetyl group; CC, disulfide link. Apoptotic effect of peptides (10 μ M) was analyzed in H460 cells.

(C) Induction of apoptosis of MDA-MB435 cancer cells by Nur77 peptides. MDA-MB435 cells were exposed to the indicated peptide (20 μ M) for 16 hr and apoptosis was determined by annexin V staining. The bars represent means \pm SD from three independent experiments.

Results: These studies demonstrate that the apoptotic effect of NuBCP is independent on cell penetrating peptides conjugated. This is also supported by the apoptotic effect of NuBCP fused with GFP in cells.

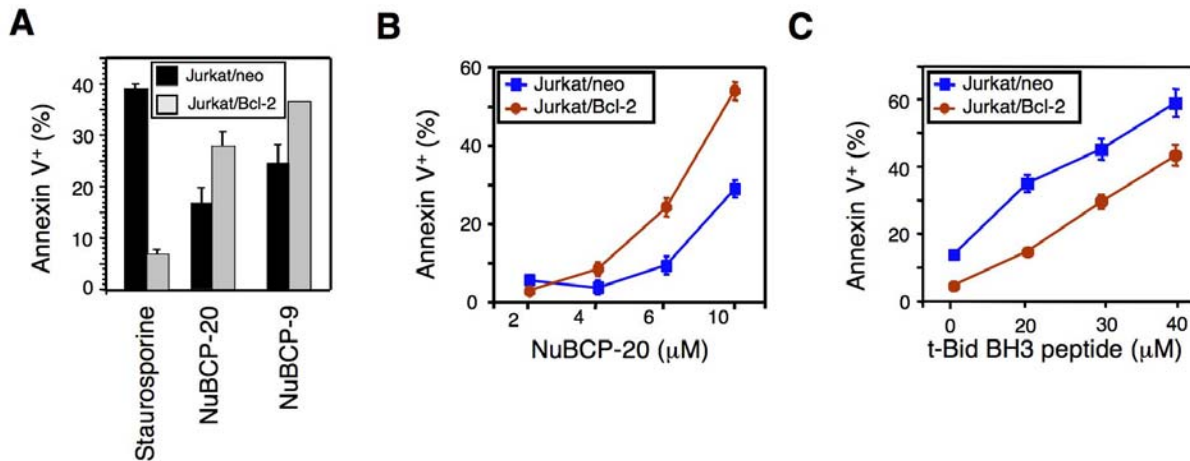


Figure S3. Bcl-2 Potentiates the Apoptotic Effect of NuBCP in Jurkat Cells

(A) Stable expression of Bcl-2 in Jurkat cells enhances apoptosis induced by NuBCPs. Jurkat and Jurkat cells stably expressing Bcl-2 were exposed to NuBCPs (10 μ M) or treated with staurosporine (0.1 μ M), and apoptosis determined by annexin V staining.

(B and C) Opposing effect of Bcl-2 in Jurkat cells. Jurkat and Jurkat cells stably expressing Bcl-2 were exposed to the indicated concentration of NuBCP-20-r8 (B) or t-Bid BH3-r8 (C) peptide for 16 hr and apoptosis was determined by annexin V staining. The bars represent means \pm SD from three independent experiments.

Results: These studies provide additional evidence that the apoptotic effect of NuBCPs depends on Bcl-2 expression. In addition, they show again that Bcl-2 exhibits dual phenotypes, inhibiting apoptosis induced by staurosporine and t-Bid BH3 peptide and promoting apoptosis induced by NuBCPs.

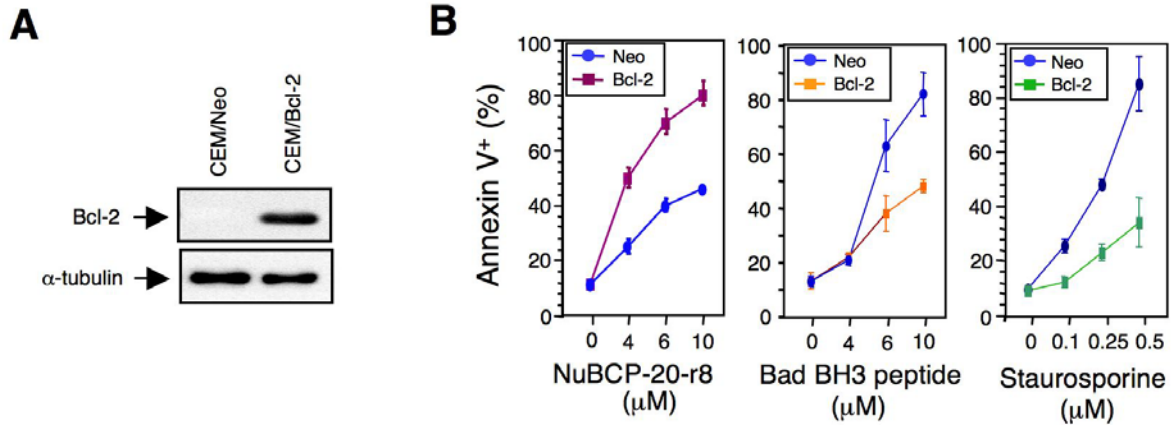


Figure S4. Stable Expression of Bcl-2 Enhances Apoptosis by NuBCP

(A) Expression of Bcl-2 in CEM stably transfected with control neo vector or Bcl-2 determined by immunoblotting. Levels of α -tubulin were used for control.

(B) CEM cells stably transfected with control neo vector (Neo) or Bcl-2 (Bcl-2) were exposed to NuBCP-20-r8 or Bad BH3 peptide, or treated with staurosporine for 12 hr, and apoptosis determined by annexin V staining. The bars represent means \pm SD from three independent experiments.

Results: These studies show that Bcl-2 expression enhances the death effect of NuBCP. In contrast, Bcl-2 expression inhibits the death effect of Bad BH3 peptide and staurosporine. Thus, Bcl-2 exhibits opposing effects depending on death stimuli.

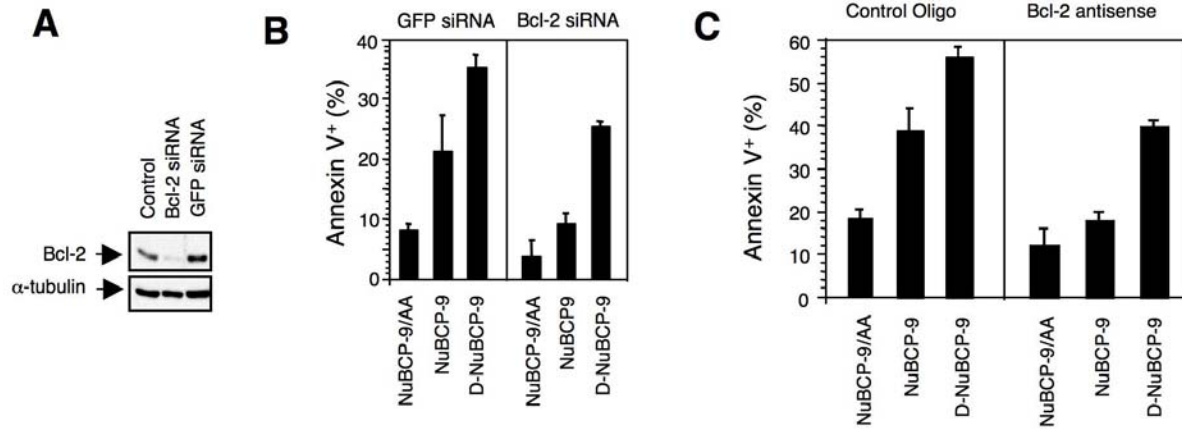


Figure S5. Inhibition of Bcl-2 Expression Suppresses NuBCP-Induced Apoptosis in H460 Lung Cancer Cells

(A) Bcl-2 expression in H460 cells transfected with Bcl-2 siRNA or control GFP siRNA determined by immunoblotting.

(B) Inhibition of Bcl-2 expression by Bcl-2 siRNA suppresses NuBCP-induced apoptosis.

(C) Inhibition of Bcl-2 expression by Bcl-2 antisense oligonucleotides suppresses NuBCP-induced apoptosis. H460 cells transfected with Bcl-2 antisense oligonucleotides or control oligonucleotides were exposed to NuBCPs (10 μM) for 16 hr, and apoptosis determined by annexin V staining. Inhibition of Bcl-2 expression by antisense oligonucleotides is shown in Figure S6. The bars represent means ± SD from 3-4 experiments.

Results. These data demonstrate that Bcl-2 expression contributes to NuBCP-induced apoptosis.

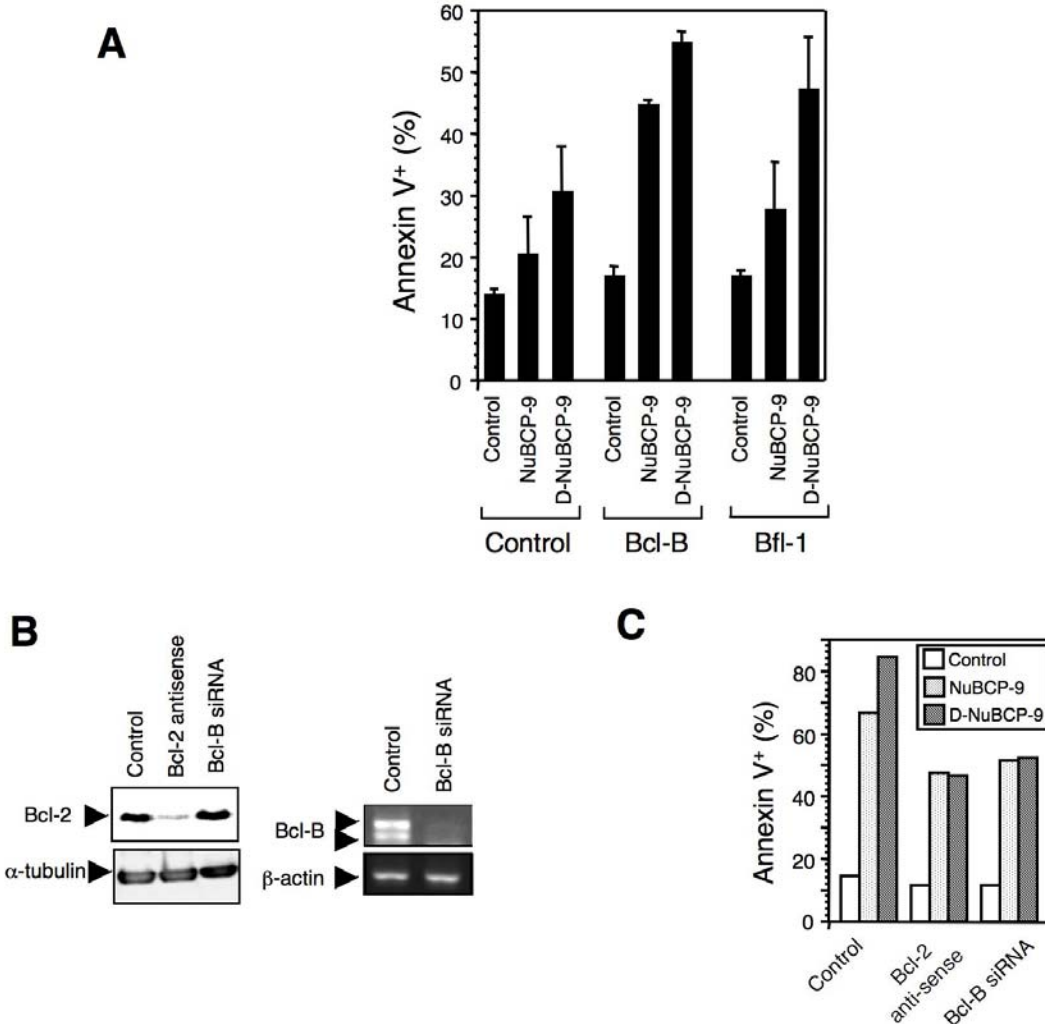


Figure S6. The Apoptotic Effect of NuBCPs Is Potentiated by Expression of Bcl-B and Bfl-1

(A) HeLa cells at 60% confluency were transfected with empty vector (Control), Bcl-B, or Bfl-1 expression vector. 12 hr after transfection, cells were treated with 10 μ M NuBCP-9 or 6 μ M D-NuBCP-9 for 16 hr. Apoptosis was determined by annexin V staining. The bars represent means \pm SD from 3 experiments.

(B) Suppression of expression of Bcl-2 or Bcl-B. H460 cells transfected with control oligo, Bcl-2 antisense oligo or Bcl-B siRNA were analyzed for expression of Bcl-2 by immunoblotting (left panel). H460 cells transfected with control (GFP) siRNA or Bcl-B siRNA were analyzed for expression of Bcl-B by RT-PCR (right panel).

(C) Knockdown of Bcl-2 or Bcl-B expression in H460 cells suppresses the apoptosis induction by NuBCPs. H460 cells transfected with Bcl-2 antisense oligo or Bcl-B siRNA were exposed to 10 mM each of NuBCP-9/AA-r8 (control), NuBCP-9-r8 or D-NuBCP-9-r8 for 16 hrs, and apoptosis was determined by annexin V staining.

Results: These studies demonstrated that NuBCP could also convert the survival phenotype of Bcl-B and Bfl-1. In addition, they show that Bcl-B expression also contributes to the apoptotic effect of NuBCP in H460 lung cancer cells.

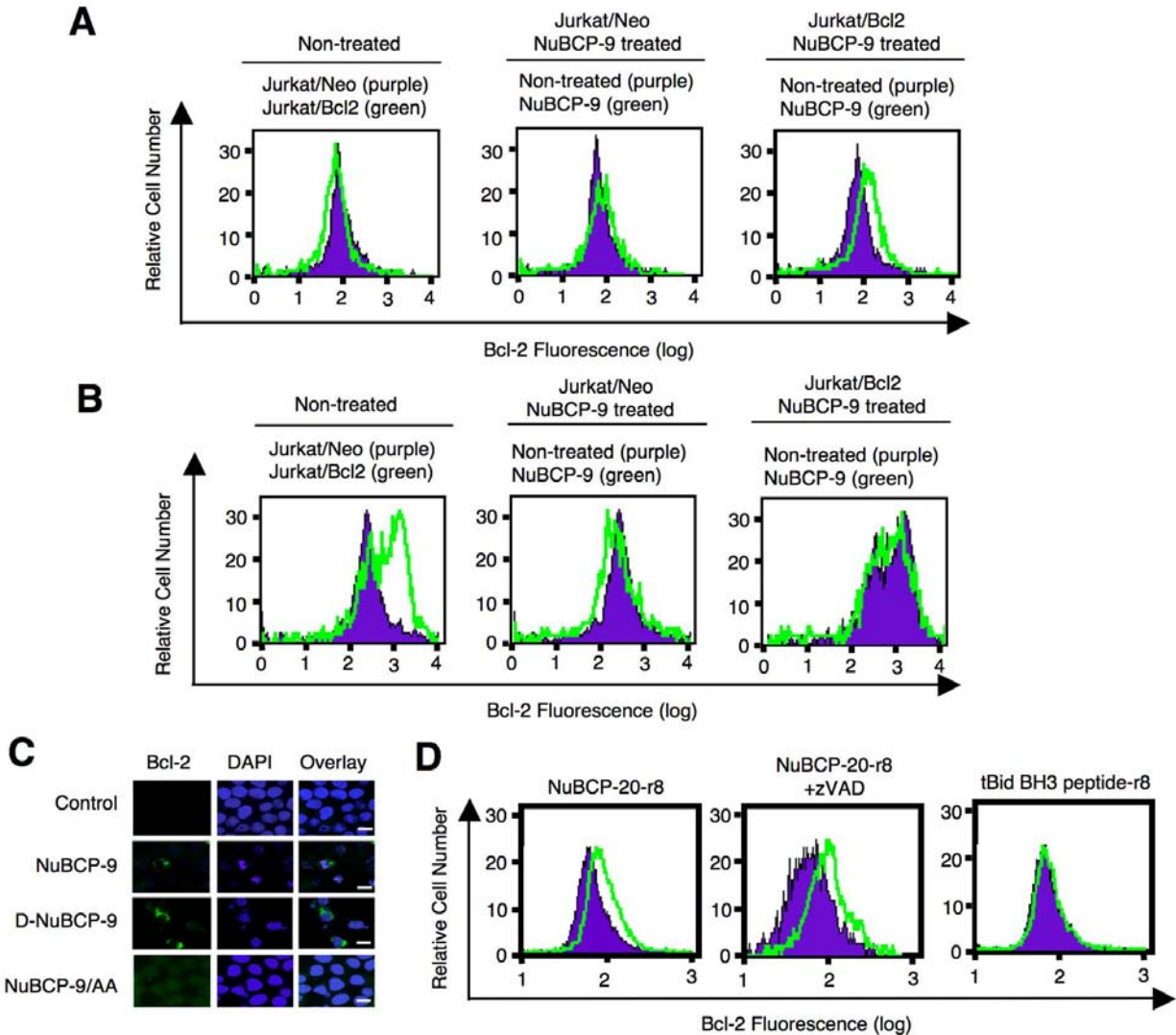


Figure S7.

(A and B) Characterization of conformation-sensitive anti-Bcl-2 BH3 domain antibody (Ab) by flow cytometry. Jurkat/neo or Jurkat/Bcl-2 cells were treated with or without NuBCP-9-r8 for 16 hr, then stained with anti-Bcl-2 BH3 domain Ab (A) or anti-Bcl-2 Ab (B), followed by SRPD-conjugated secondary Ab. The anti-Bcl-2 BH3 domain Ab detected stably expressed Bcl-2 in cells only when they were exposed to NuBCP-9. For control, Jurkat/neo cells treated with NuBCP-9-r8 did not display significant difference in staining with the anti-Bcl-2 BH3 domain Ab compared to non-treated cells. Further, rabbit polyclonal anti-Bcl-2 antibody against whole protein detected Bcl-2 protein, but not its conformational changes induced by NuBCP-9.

(C) HEK293T cells transfected with Bcl-2 were exposed to peptide (20 μ M) for 12 hr, stained with the anti-Bcl-2 BH3 domain Ab or DAPI, and examined by fluorescence microscopy. Scale, 12 μ M.

(D) Caspase inhibitor does not affect Bcl-2 conformational changes. H460 cells exposed to the indicated peptide (10 μ M) and/or 50 μ M zVAD for 16 hr were immunostained with the anti-Bcl-2 BH3 domain Ab. Bcl-2 fluorescence from peptide-treated cells (Green histogram) was compared to that from the non-treated cells (purple histogram).

Results: These studies demonstrate that anti-Bcl-2 BH3 domain antibody can be used to detect proapoptotic Bcl-2 conformation. The results also show that treatment of cells with either L-NuBCP-9 or D-NuBCP-9 results in immunostaining of transfected Bcl-2 protein by the anti-Bcl-2 BH3 domain Ab, suggesting a conformational change. Importantly, Bcl-2 conformational change does not result from apoptosis, demonstrating its role in the onset of NuBCP-induced apoptosis.

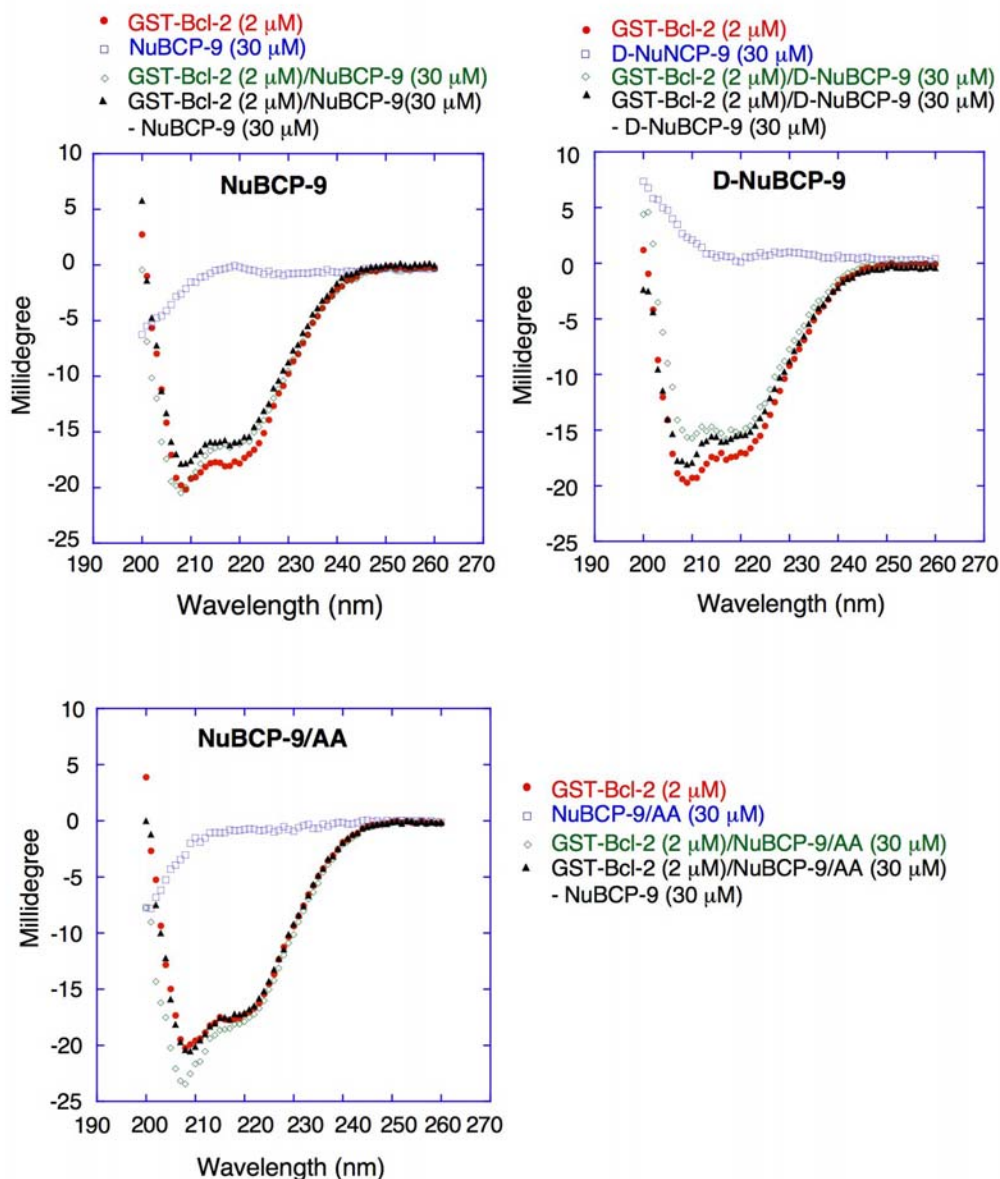


Figure S8. CD Spectra for Binding of NuBCPs to GST-Bcl-2

Samples were prepared for peptide (30 μ M) and GST-Bcl-2 (2 μ M) alone and as a mixture in PBS, pH 7.6. Peptide was diluted from a 3 mM stock solution in 30% acetonitrile/water. CD spectra for each sample were obtained in a 0.2 cm path length cell at 20°C using an AVIV 62 DS spectrometer for a wavelength range from 200 to 260 nm with a step size of 1nm averaged for 5 sec. Three spectra were averaged for each sample and corrected for background. Finally, the spectrum for the peptide is subtracted from the spectrum recorded for the mixture of peptide and GST-Bcl-2 (black) for comparison with that for GST-Bcl-2 (red).

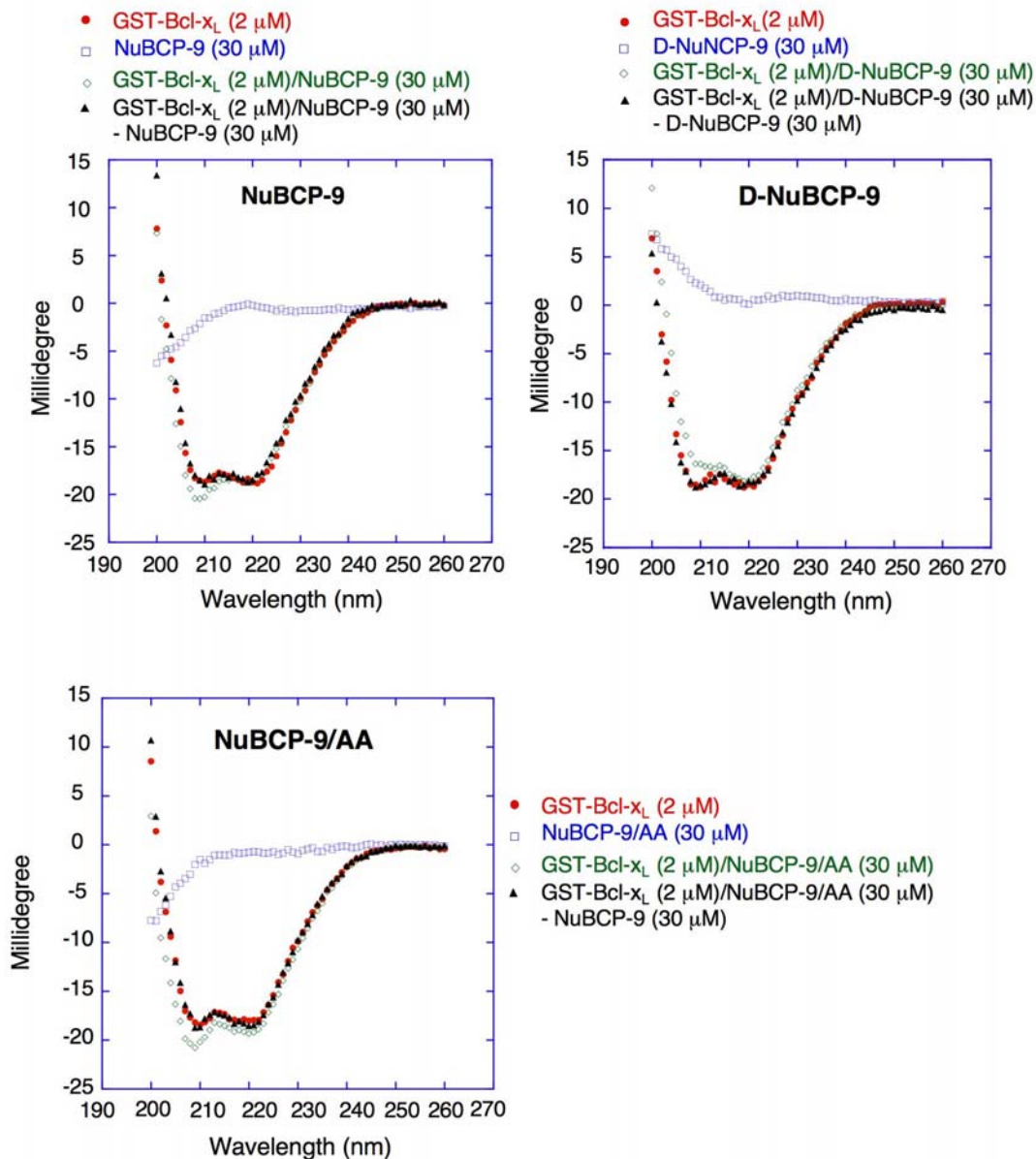


Figure S9. CD Spectra for Binding of NuBCPs to GST-Bcl-X_L

Samples were prepared for peptide (30 μM) and GST-Bcl-X_L (2 μM) alone and as a mixture in PBS, pH 7.6. Peptide was diluted from a 3 mM stock solution in 30% acetonitrile/water. CD spectra for each sample were obtained in a 0.2 cm path length cell at 20°C using an AVIV 62 DS spectrometer for a wavelength range from 200 to 260 nm with a step size of 1nm averaged for 5 sec. Three spectra were averaged for each sample and corrected for background. Finally, the spectrum for the peptide is subtracted from the spectrum recorded for the mixture of peptide and GST-Bcl-X_L (black) for comparison with that for GST-Bcl-X_L (red).

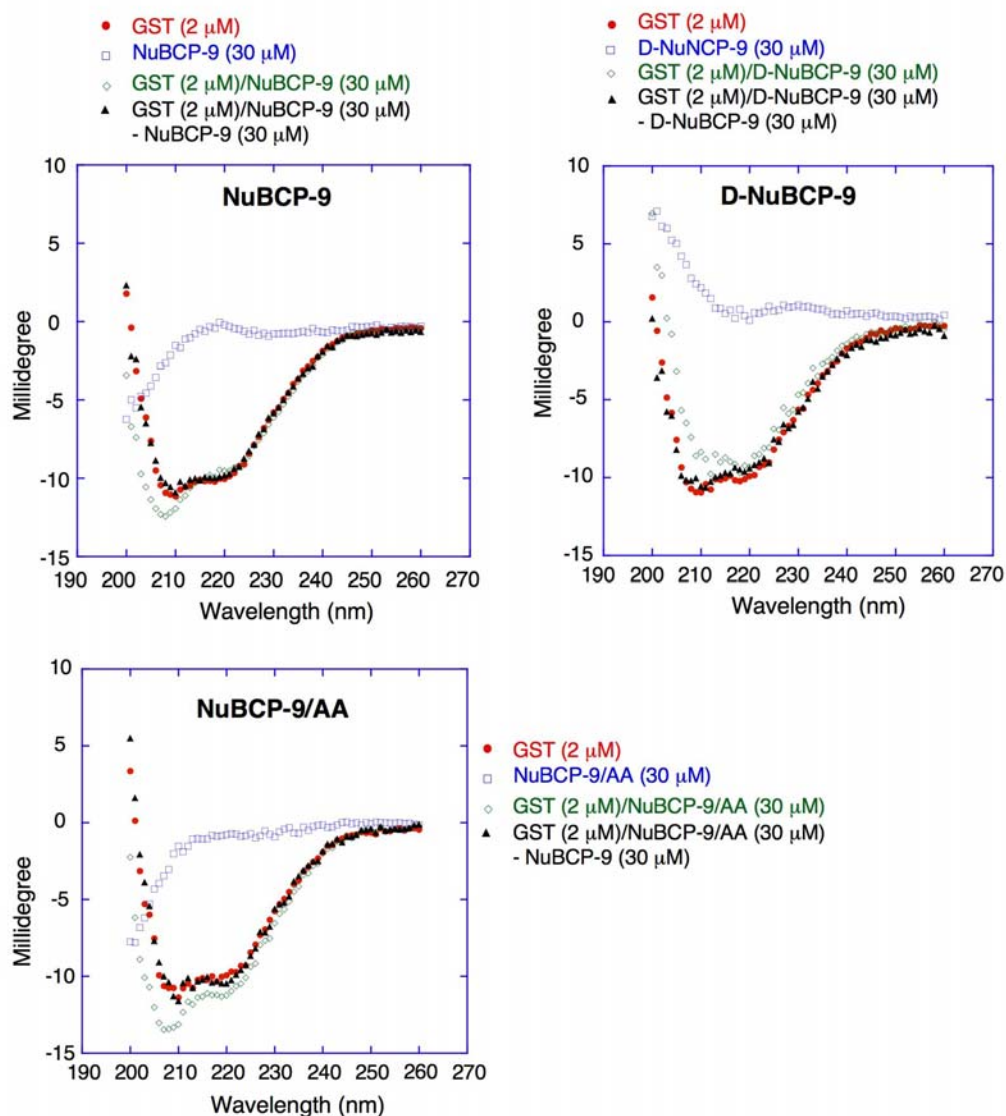


Figure S10. CD Spectra for Binding of NuBCPs to GST

Samples were prepared for peptide (30 μM) and GST (2 μM) alone and as a mixture in PBS, pH 7.6. Peptide was diluted from a 3 mM stock solution in 30% acetonitrile/water. CD spectra for each sample were obtained in a 0.2 cm path length cell at 20°C using an AVIV 62 DS spectrometer for a wavelength range from 200 to 260 nm with a step size of 1nm averaged for 5 sec. Three spectra were averaged for each sample and corrected for background. Finally, the spectrum for the peptide is subtracted from the spectrum recorded for the mixture of peptide and GST (black) for comparison with that for GST (red).

Bcl-2 Sequences

Mahagrtgydnreivmkyihyklisqrgyewdagdvgaappgaapapgifssqpghtphpaasrdpvarsp
lqtpaapgaaagpalspvpvvhltlrqagddfsrerryrdfaemssqlhltptargfatvveelfrdgwnwgrivaf
feggvmcvesvnrremsplvdnialwmteylnrhltwiqnggdafvelygpsmrpldfswlskllslalv
gacitlgaylghk

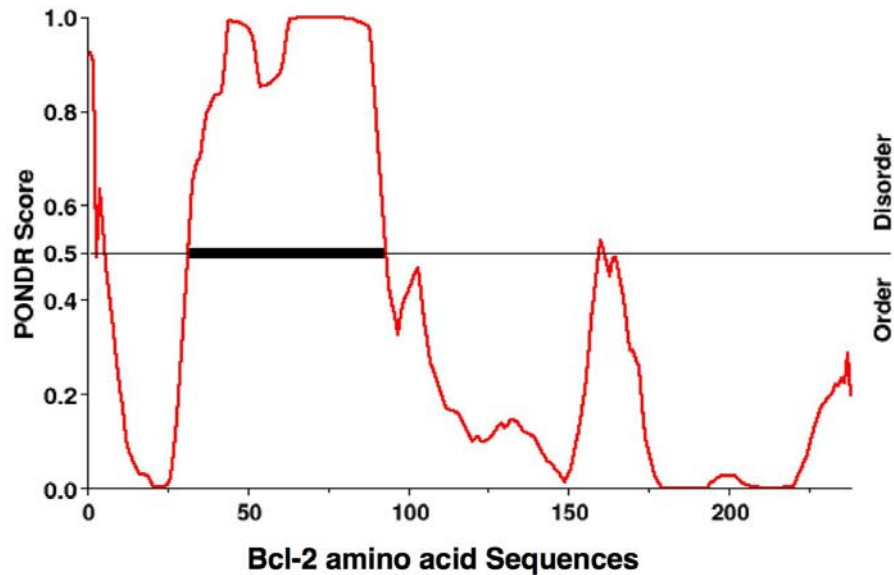


Figure S11. The Loop of Bcl-2 Is Predicted to Be Disordered

Order/Disorder scores (y-axis) predicted by PONDR VL-XT (Li et al., 1999; Romero et al., 1997; Romero et al., 2001) for Bcl-2 residues (x-axis). As highlighted by the bar, residues 33-94 of the Bcl-2 regulatory loop, all bearing scores larger than 0.5, are considered as significantly disordered.

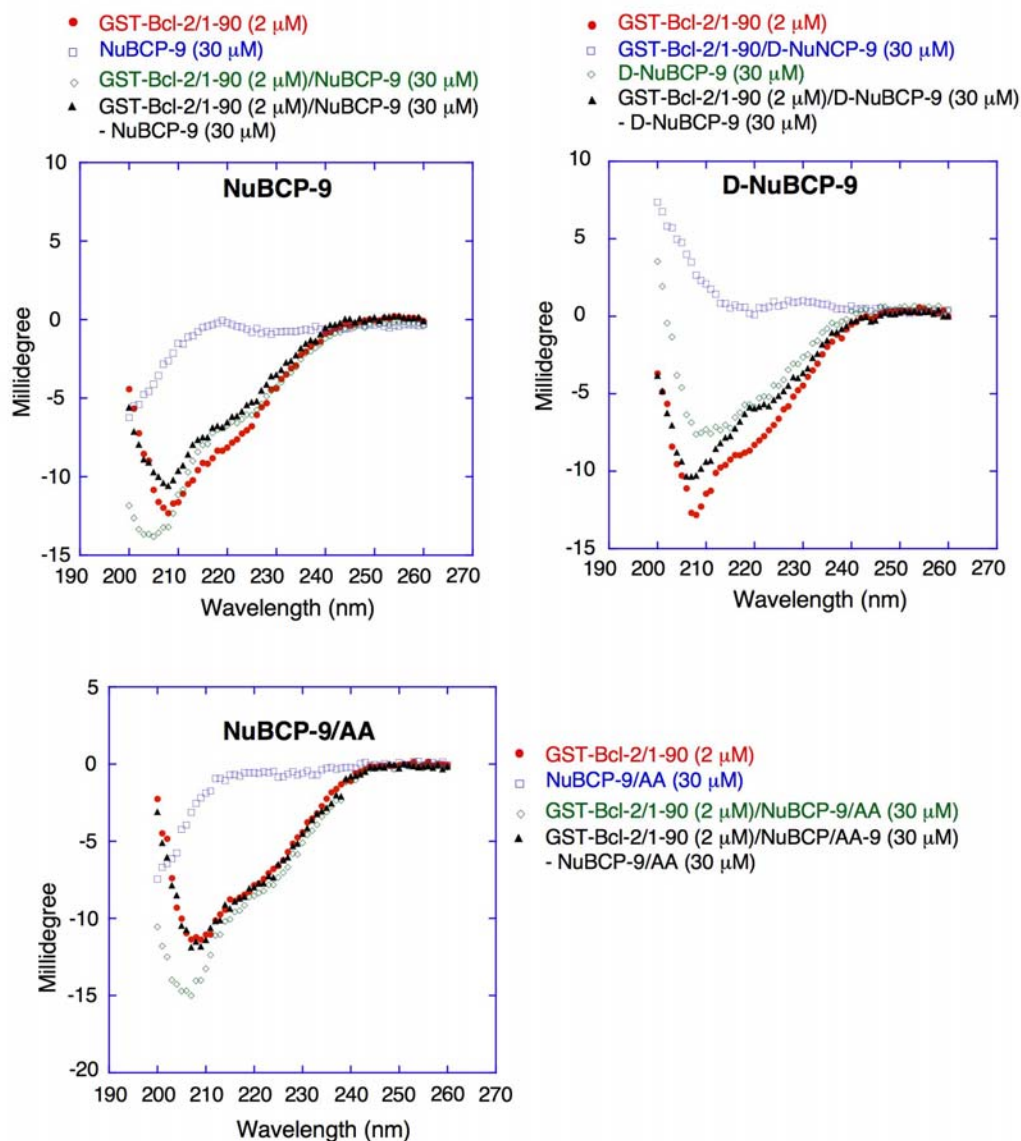


Figure S12. CD Spectra for Binding of NuBCPs to GST-Bcl-2/1-90

Samples were prepared for peptide (30 μM) and GST-Bcl-2/1-90 (2 μM) alone and as a mixture in PBS, pH 7.6. Peptide was diluted from a 3 μM stock solution in 30% acetonitrile/water. CD spectra for each sample were obtained in a 0.2 cm path length cell at 20°C using an AVIV 62 DS spectrometer for a wavelength range from 200 to 260 nm with a step size of 1nm averaged for 5 sec. Three spectra were averaged for each sample and corrected for background. Finally, the spectrum for the peptide is subtracted from the spectrum recorded for the mixture of peptide and GST-Bcl-2/1-90 (black) for comparison with that for GST-Bcl-2/1-90 (red).

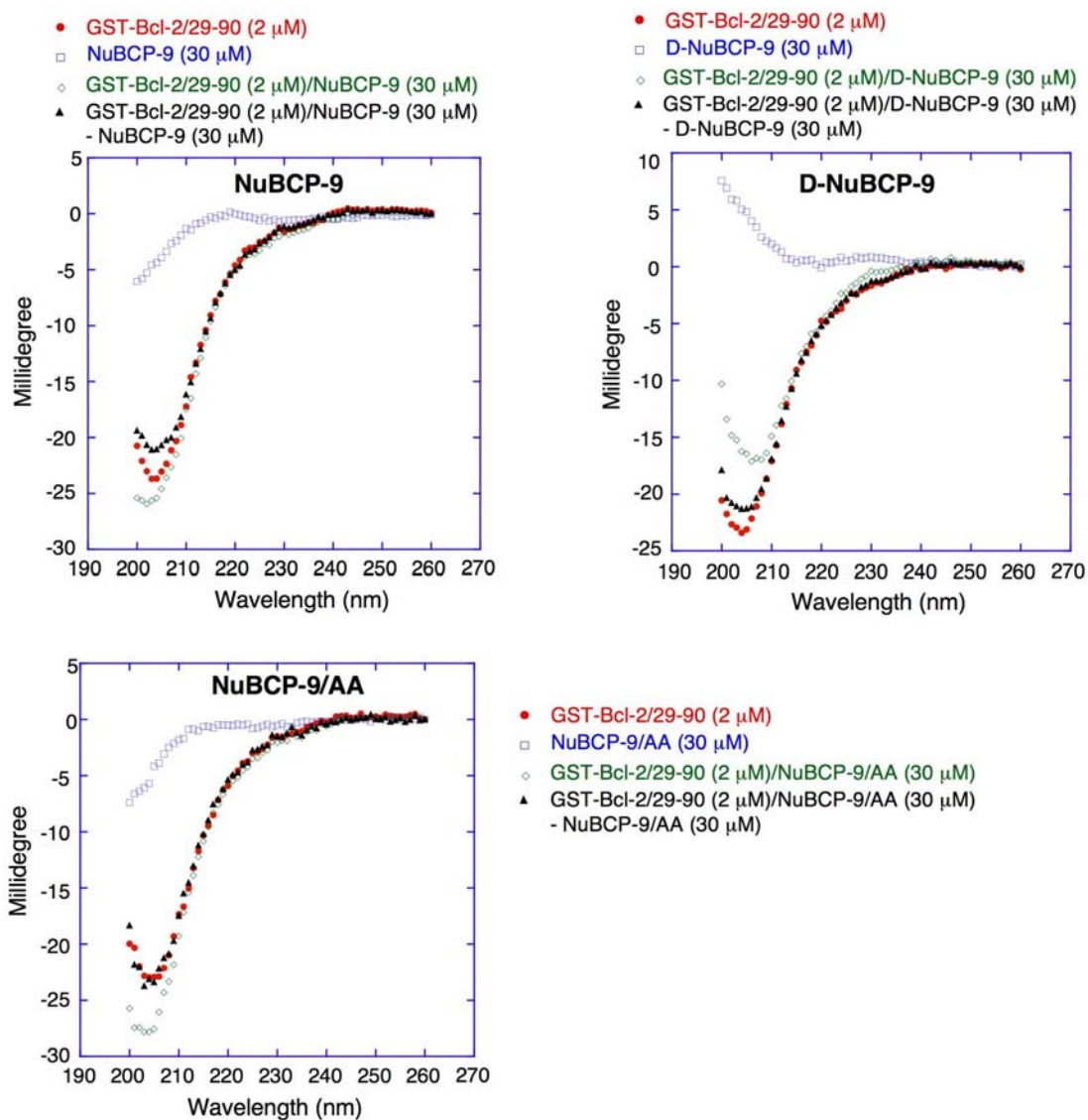


Figure S13. CD Spectra for Binding of NuBCPs to GST-Bcl-2/29-90

Samples were prepared for peptide (30 μ M) and GST-Bcl-2/29-90 (2 μ M) alone and as a mixture in PBS, pH 7.6. Peptide was diluted from a 3 μ M stock solution in 30% acetonitrile/water. CD spectra for each sample were obtained in a 0.2 cm path length cell at 20°C using an AVIV 62 DS spectrometer for a wavelength range from 200 to 260 nm with a step size of 1nm averaged for 5 sec. Three spectra were averaged for each sample and corrected for background. Finally, the spectrum for the peptide is subtracted from the spectrum recorded for the mixture of peptide and GST-Bcl-2/29-90 (black) for comparison with that for GST-Bcl-2/29-90 (red).